NTNU – Trondheim
Norwegian University of
Science and Technology

Solar driven Power production using CO2 as working fluid

Geping Zhao

Sustainable Energy
Submission date: Januar 2015
Supervisor: Trygve Magne Eikevik, EPT

Norwegian University of Science and Technology
Department of Energy and Process Engineering

Preface

A big part of this report, which is the written work of my Master thesis at the Norwegian University of Science and Technology (NTNU), Department of Energy and Process Engineering, was completed during my exchange period in Norway. The subject of this research and thesis was discussed and determined with my supervisor Prof. Yong Li from Shanghai Jiao Tong University and Prof. Trygve Magne Eikevik from Norwegian University of Science and Technology. During my first semester in NTNU, a project related to this subject was completed by me with Prof. Trygve's help. Afterwards, in my second semester in NTNU, I took this thesis which accounts for 30 credits of my master degree in NTNU, the study program of which was "Sustainable Energy Research". The title of my master thesis is "Experimental and computational research on the feasibility of solar driven power production in Rankine cycle using CO_2 as working fluid".

This exchange period had been an extraordinary experience for me, both academically and socially. During the studying period, I have got in touch with a wide range of knowledge from lectures and instructions from different professors and advisors, especially during my project and thesis period. The experimental research, as well as the studying of the simulations software Dymola, was very specifically instructed thanks to NTNU and SINTEF staffs. This experience of studying has made me be of more knowledge about this research field and cultivated my ability to solve academic problems in the future. I acquired certain levels of insights within the sustainable energy issue and the global current situation of it.

Doubtlessly I would first give my thanks to my supervisor Prof. Trygve at NTNU, for the thorough and detailed assistance he offered me when I have difficulty carrying on the research. His constructive feedback kept me on the proper path throughout the whole process of my thesis. In the meantime I would also extend my gratitude to Prof. Yong Li at SJTU, for his further valuable suggestions and guidance at the part of my

thesis writing. There are other persons I would gladly give my thanks to, for all kinds of help they offered me, including Zhequan Jin who taught me many skills in using the software of Dymola, Mr. Eugen who provided me with help of the installation and license permit of the computational software, and Ms. Maria Alonso who helped me get the initial understanding of the system and its principles.

Last but not least, I give many thanks to my fellow students who had been in Norway together with me as exchange students. I am more than grateful for this wonderful experience and memory.

Shanghai, November 2014

Geping Zhao

Abstract

This thesis work, titled as “Experimental and computational research on the feasibility of solar driven power production in Rankine cycle using CO_2 as working fluid”, involves the study of Rankine cycle in power production and CO_2 characteristics in heat transfer, especially its features in super-critical phase. The conceptual construction of solar collector is not actually installed, but a heat pump cycle was added in order to serve as a relatively low input heat source temperature. The proposed system under this concept was operated and the corresponding test results were collected and analyzed. According to the test results and the analysis, the feasibility of this system was abundantly confirmed. The system shows a great and promising potential in application.

However, as the components of the test rig, especially the expander and pump did not seem to be functioning properly and stably when the CO_2 working fluid was under higher temperature and higher pressure. Therefore, a computational model was established in Dymola software and validated according to the acquired data from the tests, for the sake of extending the working condition virtually. In the simulation, the input heat source temperature was raised from 80 ℃ to as high as 200 ℃, the consequences of which indicated that the power production climbed significantly under such working condition. As a conclusion, the simulation proved that it is of great value to modify this test rig for better performance under further working condition and the future of its application is very promising.

Abstrakt

Denne avhandlingen med tittelen som "Experimental og beregningsorientert forskning på muligheten for solenergi drevet kraftproduksjon i Rankine syklus med CO_2 som arbeidsmedium", omfatter studier av Rankine syklus i produksjon og CO_2-effekt egenskaper i varmeoverføring, særlig dens funksjoner i super -critical fase. Den begrepsmessige konstruksjon av solfanger er faktisk ikke er installert, men en varmepumpesykluscycle ble tilsatt for å tjene som en forholdsvis lav inngangsvarmekildetemperaturheat source . Det foreslåtte system i henhold til dette konsept ble operert, og de tilsvarende testresultater ble oppsamlet og analysert. Ifølge testresultatene og analyse, ble gjennomførbarheten av dette systemet rikelig bekreftet. Systemet viser en stor og lovende potensial i søknaden.

Imidlertid, ettersom komponentene i testrigg, spesielt ekspanderen og pumpen ikke synes å funksjonere riktig, og når CO_2 stabilt arbeidsfluid var under høyere temperatur og høyere trykk. Derfor ble en beregningsmodellmodel etablert i Dymola programvare og validert i henhold til de innsamlede data fra testene, av hensyn til å utvide stand nesten. I simuleringen ble inngangs varmekilde temperaturen hevet fra 80 grader til så høyt som 200 grader, konsekvensene av som indikerte at kraftproduksjonen klatret betydelig under en slik stand. Som en konklusjon, simuleringen viste at det er av stor verdi for å endre denne testrigg for bedre ytelse under videre stand og fremtiden for sin søknad er svært lovende.

Table of contents

1. Introduction

1.1 Background

Since the very primary development of technology many years ago, humans have been devoted to perfecting all kinds of living conditions due to natural chase for a better life standard. Electricity supply, heating demand and power production are all important in our daily life. If we take a good look at the whole history of utilizing energy, the most dominating resources have been fossil fuels such as coal, oil and natural gas. These fossil fuels obviously had great advantages and played a very important role in the early period of industrialization. As the development went further and deeper, however, it began to bring up people's awareness that fossil fuels have their severe disadvantages and negative effects.

The development of human being has gone through a very long period of utilizing all different kinds of energy supply. With the extremely rapid development of technology in the past hundreds of years, modern human life can't exist or maintain without a constant and sufficient supply of electricity and power. A good resource of power supply must satisfy these criteria: stable in long-term operation, capable of bearing peak and valley demands, and efficient in forms of energy conversion. The major method of power generation is based on technology of fossil fuel combustion such as oil, natural gas, coal, etc. However, as the fossil energy is an un-sustainable resource and will eventually run out, it is absolutely necessary and urgent to develop other methods for substitution of power production. One of the most promising power generating methods is by taking advantage of low temperature surplus heat recovery. In industry fields, a huge amount of surplus heat, for instance rejected heat to the ambient, is available. Therefore, the concept of using such kinds of surplus heat for the purpose of electricity generation is of great interest. Researchers have developed a variety of methods for utilizing such surplus heat, one of which is based on an operation using suitable working fluid in a Rankine cycle.

1.2 Objective

The purpose of this research was to examine the performance of the proposed test rig set-up in a Rankine cycle simulating solar energy as heat input and utilizing CO_2 as working fluid for power generation. The first objective was to analyze the test results and confirm the feasibility of this system. However, with consideration of limits of the test rig, the working condition has the need of extension. Therefore, a computational model for simulation of this system was established for validation. After validated, the computational model was used for simulation of different working conditions which cannot be carried out in the real system. As a result, the second objective was to evaluate the performance of simulation model. With the experimental data recorded and analyzed, and results of simulation calculated, some conclusions were made and illustrated.

1.3 Outline

Chapter 1 Introduction of the system

Chapter 2 Research front and status

Chapter 3 Objects of this thesis

Chapter 4 Proposed test rig and the results

Chapter 5 Modeling and validation

Chapter 6 Analysis and conclusion

1.4 Future work scope

In this thesis, several series of tests were carried out in order to examine the feasibility of the proposed system in power generation with Rankine cycle utilizing CO_2 as its working fluid. The critical point in this research was to testify the suitability of supercritical phase CO_2 in Rankine cycle. Due to the limits of the corresponding components, when operating under heat source temperature higher than 100 ℃, the system showed unstable features. Therefore, a simulation model was established to be validated. In the simulation the performance was examined after the extension of its working condition. The potential of this system operating under heat source temperature as high as about 200 ℃ was proved to be considerably promising. Considering the possibility of utilizing this system in larger scale, this research has significant meaning for the future.

If bringing a further step of this research is of necessity, a better system consisting of components with better strength and more suitable properties in handling high pressure and high temperature is to be built. Moreover, some further theoretical analysis of the ideal situation in supercritical phase CO_2 is also to be proposed.

2. Research front and status

In conventional industry fields, fossil fuel is always the most widely used option in power generation processes. But as is mentioned above, the fossil fuel is a kind of limited and non-sustainable resource and will lead us into the crisis of energy shortage, not to mention the side-effects such as global warming and air pollution. Therefore, new sustainable energy like wind power and solar power has attracted people's attention. The applications of solar energy in power generation and in heat production or refrigeration have become one of the research fronts in utilizing solar power. For the purpose of studying Rankine cycle powered by solar energy, the working fluid of

which is supercritical carbon dioxide, a model and numerical investigation is developed to predict the performance of this cycle in the article[1].

In the design of this system, solar heat is collected by the evacuated solar collector and used to heat up CO_2 temperature into supercritical state. Supercritical CO_2 then drives the engine of the Rankine system, producing power output in this system. Afterwards, the CO_2 of lower pressure is expelled from the turbine and cooled down in the heat recovery system or the heat exchanger. The rejected heat here can be easily utilized as heat source for absorption refrigerating machine, air conditioning or boiling water, etc. At the end, CO_2 is pumped back into the higher pressure condition and the cycle recommences. The intention of this design is to satisfy the heat loads of commercial facilities, buildings, dwellings and other equipment that can obtain benefits from an independent power or heat source.

A thermodynamic analysis is raised and presented in this paper. In the simulation process evaluated under simplified conditions, a few assumptions are made as below:

1) The solar energy collector is facing south and absorbs solar radiation all day, and is kept dust-free.
2) Thermal resistance is ignored among the selective surface of the evacuated solar collector.
3) Supposedly supercritical CO_2 is fully distributed within all the tubes and components.
4) There are no friction loss in the solar collector and heat exchangers.
5) The pressure of the pump outlet is set at 9.0 MPa which is a close value to the experimental data. The pressure drop of the turbine is also set as constant of 2.5 MPa.
6) No leakage or thermal loss exists in the CO_2 loop.

For estimation of the thermodynamic and transport properties of CO_2, a Program

Package of Thermo-physical Properties of Fluids database version 12.1 (PROPATH 12.1) is applied in this paper. The performance of this system is determined and examined by solving a set of equations simultaneously. The results are listed below.

The temperature of supercritical CO_2 at the outlet of the solar collector is up to 217.4° C in summer and 137.0° C in average. At the turbine outlet, it is 181.6° C in summer and 143.1° C in average. For the outlet of heat exchanger, the figures are 140° C and 115° C, respectively. There is no argument that it can be utilized as heat sources for water boiling for domestic use or absorption refrigeration. Furthermore, the calculation of the annually averaged power generation efficiency is 22.2% and heat recovery efficiency is 68.0%. Another finding is that the power generation efficiency decreases following the increase of the solar energy collecting area, due to the overall heat capacity increment. However, the total power output will rise as the enlargement of solar collecting area. In other words, it is of great value to optimize the parameter of the area of solar collector. In the heat recovery components, when the area of heat exchangers increases, the cycle temperature falls, resulting in a drop of the electric power and heat outputs.

This numerical research has revealed a few conclusions:

1) The consequences of this simulation based on formulation study indicate that the power generation efficiency and heat recovery efficiency is around 20.0% and 68.0%, respectively.
2) There are several independent parameters such as the climate, the collector area, the heat exchanging area, water temperature and water flow rate of the system. These parameters need to be balanced and optimized based on the overall performance of the system.
3) The influence of the water flow rate can be neglected in the cycle performance.
4) A more detailed model of transient simulation is needed for further study and understanding of the CO_2 Rankine cycle performance.

In order to utilize solar energy in power generation systems, a Rankine cycle is provided in the article[2], trying to take advantages of solar power collectors by providing relatively stable heat source. In addition, the availability of achieving a cogeneration of heat and power in this cycle is very well-developed. In this paper, CO_2 is taken as the working fluid within a Rankine Cycle and is converted into high-temperature supercritical state, thus driving a turbine and produce electrical power. As this cycle is operating, it also recovers or rejects an abundant amount of thermal energy, which can play a role as heat source for an absorption refrigerator, hot water supply or air conditioning for indoor environments. A series of experiments is constructed and established for the purpose of investigating the behavior of the CO_2-based Rankine Cycle. The efficiency and potential of such applications of this CO_2-based system is analyzed and discussed.

The basic principles of the CO_2-based Rankine Cycle are that an evacuated solar collector is used to heat CO_2 in heating channels, making CO_2 become supercritical state and drive the turbine in the Rankine system and provide power output. Afterwards, the CO_2 expelled from the turbine is cooled down in the heat recovery system and the heat rejected is utilized for absorption refrigerating bed or other uses. In this case, a heat and electric power cogeneration system is established and the performance of it is investigated. It has to be pointed out that the heart of the CO_2-based Rankine Cycle system is the solar collector, the characteristics of which are essential in such systems. A higher temperature of CO_2 will make the whole system function in better conditions. Therefore, efforts were made to measure the cycle temperatures for the sake of studying the feasibility of such systems in this paper.

Supercritical CO_2 is actually in-between the liquid phase and the gas phase of it, so it is difficult to determine whether a turbine for gas or for liquid should be used for such working fluids. Meanwhile, instead of a usual turbine, a pressure relief valve was used in the experiments and provided various extents of opening for the cycle loop so that

the pressure drop can be simulated and the power production can be estimated based on thermodynamic theories. The following thermodynamic equation 1 is used to calculate the power generation from the turbine.

$$W_{power} = m_c \eta_{is} \eta_{gen} (\frac{k}{k-1}) RT_1 \left[1 - (\frac{P_2}{P_1})^{\frac{k-1}{k}}\right]$$

Equation 1

Where m_c is the mass flow rate of CO_2, R is the gas constant, k is the ratio of the specific heat at constant pressure and constant volume, T_1, P_1 are the temperature and pressure at the turbine inlet, P_2 is the pressure at the turbine outlet.

During the tests in Japan, the CO_2 temperature reaches up to about 194.0° C at 12:00, then drops gradually with time. The average temperature at the outlet of solar collector from 10:00 to 17:00 is about 185° C, which makes the thermal energy collection easy and achieves power generation in the turbine. At the outlet of the valve, the CO_2 temperature is about 160.0° C, and such a heat source can be effectively utilized for boiling water, absorption refrigerating and air conditioning. The results from the solar collector show an efficiency of 62%, which explains why a relatively high temperature of 185° C is achieved at the collector outlet. The estimation of power output and the pump work is about 0.82kW and 0.15kW, respectively, and the heat recovery achieved is about 4.20kW. The power generation efficiency is estimated at 0.16 and the heat recovery efficiency is 0.82. The overall results obtained in the experiments prove that supercritical CO_2 can effectively collect heat in the solar collector then achieve heat recovery and power generation. The CO_2-based Rankine Cycle operates under supercritical region throughout most of the test time, and achieves a reasonable efficiency of power generation and heat recovery, the potential of which is very promising in various aspects of applications.

In the article[3], experimental results are analyzed to discuss the potential of the

application of solar-driven powered cycle in terms of a combined electricity and heat generation.

In the experiments, the total amount of CO_2 charged into the cycle as working fluid is about 6.0kg. Meanwhile, the inlet water temperature and flow rate are controlled at 30.0° C and 0.230kgs^{-1}, respectively. The CO_2 outlet temperature of the solar collector reaches up to 180.0° C and 140.0° C in summer and winter, respectively. The average outlet temperature of them is 160.0° C in summer and 120.0° C in winter, which is promising. It has to be addressed that the high pressures reach up to 8.0MPa and low pressures are around 6.0MPa.

The experimental results show that this CO_2-based cycle is capable of providing a stable power output and heat source, the thermodynamic efficiency of which is COP_{power}=0.053 and $COP_{heat} = 0.353$ in winter.

With an industrial low-grade steam as heat source, an analysis of supercritical power cycle using CO_2 as working fluid is presented in details in the article of "Analysis of a carbon dioxide supercritical power cycle using a low temperature source"[4]. This analysis is divided into four major parts: energy analysis, exergy analysis, finite size thermodynamics and surface calculation of the heat exchanger. In the results an optimized high pressure is determined for each part of it. Moreover, it is proved by the analysis that the net power output from the limited heart source has no impact on the energy analysis, and the power output decreases the exergy efficiency while increasing the heat exchanger's surface.

One advantage of some proposed cycles using binary mixtures or supercritical pressure is that the low-grade heat sources are applicable. In this paper, the focus is on the supercritical cycle considering the high potential of it and the lack of studies as well. Two configurations are looked into and the only difference of it is the presence of a regenerator. The following reasons describe the benefits of choosing CO_2 as the

working fluid:

1) The critical properties of it are highly suitable for the external conditions in this paper.
2) Environment-friendly as CO_2 is, the ozone depletion potential is 0 and a global warming potential is 1 over 100 years.
3) The cost is low and the safety is assured.
4) The compatibility is also admirable.
5) Favorable thermodynamics and transport properties.
6) The thermo-physical properties of CO_2 are already well analyzed even in the supercritical area.

The results of this parametric study are presented below. The parameters are set at constant value as described. The high pressure varies between 9 and 15MPa. The variation of the net power output is independent to the non-dimensional power coefficient α. A maximum specific power output is obtained as 18.8kJ/kg at the pressure of 11.5MPa. However, when the system with regenerator operates at 11.4MPa a very promising compromise is achieved with both the specific net power output and the thermal efficiency. On the contrary, the results of the exergy analysis are depending on the values of both the parameters of pressure and α. It is revealed that when the power output extracted from the heat source increases, the exergy destruction also increases. As for the total heat exchange surfaces, the total surface area increases with α and is significantly high.

In another article in related fields[5], an improvement is carried out in conventional Rankine power cycle. Instead of using a mechanical pump, a thermal driven pump is applied to provide the pressure increment of the fluid, which can enhance the performance of net power output and reduce the operational and maintenance cost.

The thermal driven pump is a component that utilizes the thermodynamic phenomena that the pressure of a certain fluid will increase as the temperature rises. Therefore, it

is applicable to use a thermal driven pump to create a pressure increment within fluids.

With analysis of the energy balance for Rankine cycle, using CO_2 as the working fluid of the system, the pressure can be raised by several bar for a relatively small temperature increment(10-25° C), thus making it possible to increase the pressure using low temperature heat source(60° C). In other words, a novel supercritical CO_2-based Rankine cycle is proposed without using mechanical pump. The theoretical thermodynamic analysis proved that this design is favorable in terms of avoiding the requirement for maintenance, noise and vibration, installation and operating costs of a pump. However, with substitution of a thermal driven pump, a heat source will be necessary in order to provide a driving force for the heating process.

In the article[6], a study of SCRS (Solar CO_2 Rankine System) is carried out to analyze the performance of CO_2 as working fluid in a Rankine System under solar heat supply. This system can provide both electricity output through a turbine and heat supply through the heat recovery system.

In recent years, solar energy related technologies have attracted much attention in the industry field, one important aspect of which is about transforming solar power into electric power generation. For it is of great benefits to use solar energy in a Rankine cycle for the purpose of power generation, a SCRS system is built and tested, with the working fluid of CO_2. Since CO_2 can be effectively converted into the supercritical state with high temperature, the properties of supercritical CO_2 is sufficiently taken advantage of in this research.

Instead of a turbine, a pressure relief valve is installed in the system to determine the potential work output. The effective area of the solar collector in this system is 9.6 m^2. In this research the SCRS performance is analyzed on the basis of daily, monthly and yearly experimental data. It is indicated that a trans-critical Rankine cycle is

effective in power generation and heat supply. The efficiency of solar heat collection is ranged around 70%, and the power generation efficiency of the SCRS is determined at 8.78%-9.45% (the theoretical maximum is above 10.7%-11.6%). When compared with the solar cell technology (usual efficiency of which is around 8.20%), SCRS has some advantages in the aspect of effectiveness and optimization. In addition, when a suitable real turbine is used in substitution of the pressure relief valve in this system, the efficiency could be more optimized. In other words, the potential of the CO_2-based solar Rankine system is very promising and needs to be further exploited.

The mutual influence or interactions of working fluid properties is discussed in the article of "Thermodynamic and heat transfer implications of working fluid mixtures in Rankine cycles"[7]. The performance of Rankine cycles, heat transfer and cycle variations is demonstrated, and the working fluid mixture is introduced as an additional discussion. Experimental results are showed to reveal the potential for improvement of efficiency and capacity. If liquid sub-cooling is allowed, the flexibility of it can be achieved. This analysis offers new perspectives and solutions to old and new energy conversion applications, including heat pumping, heat transformation and power generation. However, the situation is complicated when it comes to that the advanced cycles require effective heat and mass transfer surfaces as well as new heat transfer concepts.

In another inspiring article[8] an Off-design operation simulation is run in order to compare the performance and effectiveness of two types of working fluid: R-123 and CO_2. In conventional situations, most of the power production methods utilizing surplus heat are by the steam process. Although this process is easily found in nuclear, gas- or oil-fired, biomass-fired and even solar power plants, it still suffers from high capital cost and poor efficiency when it comes to medium or low temperature heat sources (below the temperature of 400 ℃). However, if an organic Rankine cycle is established in such situations, it will be of great benefits in improving efficiency, reducing capital costs and operating costs for low-temperature heat sources. The

working fluids of organic Rankine cycle are organic compounds in the hydrocarbon or halocarbon families, which are widely used in refrigeration processes. Also, CO_2 is another natural option for this technology. Due to the properties of CO_2 such as high working pressure and low critical temperature, it can operate at a condition of around 100 bars at heat absorption, thus giving a possibility to reduce the size of components and the costs of investment. Besides, no phase change (only supercritical phase exists) also means easing source integration.

In this simulation model, research is based on a refrigerant property library developed by SINTEF Energy Research and NTNU. For CO_2 (R-744) properties, the Span-Wagner equation of state is used, while for R-123 the Chan-Haselden equation of state is applied. The high-side pressure and mass flow rate of the working fluid being set, with specified heat transfer coefficients (HTCs), the model solves the heat exchangers, area and heat sink, and source specifications as well.

The simulation results for the two processes are listed below. The output for the R-123 and CO_2 cycles is 4.1kW and 4.9kW, respectively, normalized with the work output in the design point (air source temperature=100℃ and mass flow air=1kg/s). The simulations at the design point indicate a 20% higher work output for the CO_2 cycle than the R-123 cycle. In addition, it is very obvious that the R-123 cycle is vulnerable for reduction in available heat; either it is a reduction of temperature in heat source or mass flow. If the amount of heat added is reduced, the R-123 cycle will drop directly into the non-feasible area. The reason is the optimal operating point for the R-123 cycle is with the inlet of the expander at the saturation line. The outlet of the evaporator will always be wet if the amount of heat transfer is reduced. Considering the sensitivity to heat source temperature reduction in the organic Rankine cycle, some superheat at the inlet of the expander is reasonable, though it means having to lower the work output. Results from simulations indicate that at 5 to 10 K superheating, the work output reduction is bearable (about 0.2% reduction for 5 K superheating and 0.4% reduction for 10 K superheating). The CO_2 cycle can

tolerate much more significant reduction in available heat, but the work output will drop rapidly. When the available heat amount is increased, both cycles will operate at feasible conditions, but the increase in work output is different. The work output from the CO_2 cycle increased more than the R-123 cycle, but not a decisive distance. When the mass flow of air changes, generally the CO_2 cycle adapts better to small changes, but the gradient of the increment will rapidly be reduced compared to the R-123 cycle. When the air temperature is increased, it is the CO_2 cycle that performs better with both small and big increments.

In conclusion, the ORC is more sensitive to reduction in available heat, and will get droplets with only small droplets, thus some superheating is reasonable. With small increments in the available heat source, the CO_2 cycle also have a marginally better response, which indicates that it is more robust and less in need of detailed control.

3. Objectives

With the research front and current situation, the objectives of this thesis were determined. The first objective was to study the feasibility of the proposed solar energy powered Rankine cycle using CO_2 as its working fluid. According to the test results and analysis, it was clearly indicated that the proposed system is capable of power generation with a low-temperature heat source input.

The second objective was to extend the testing conditions of the proposed system due to the limits of it. Resulting from that some certain equipment and components were not suitable with higher intensity in dealing with high pressure and high temperature situation, the input heat source temperature was set at 80 $^{\circ}C$. In order to extend the conclusion, it is necessary to build a computational model and verify it so that the boundaries of the system can be virtually pushed further. After extension of the testing conditions, especially the variable of input heat source temperature can be raised to a

higher figure, leading to more feedbacks through simulation. On the basis of simulation results, this system and its potential can be more sufficiently analyzed and concluded.

4. Test rig and results

4.1 Introduction of the test rig

The system consists of four loops, which are the expander cycle as the primary process, the air loop working as the heat source, the ethylene-glycol loop as the heat sink, and the heat pump loop as supplementary circuit.

In this system a direct heat source is utilized as to serve as the input heat energy. It functions equally as a solar collector.

4.2 Overview of the test rig system

The detailed system diagram is shown in Figure 1, including all four loops of the system and the whole set of components. However, this test rig is quite large and it will be inconvenient for explanation of the working principles of this system. Therefore, a simplified system diagram is presented in Figure 2, with non-crucial components hidden and major components of the four loops remained, allowing simplification of explanation.

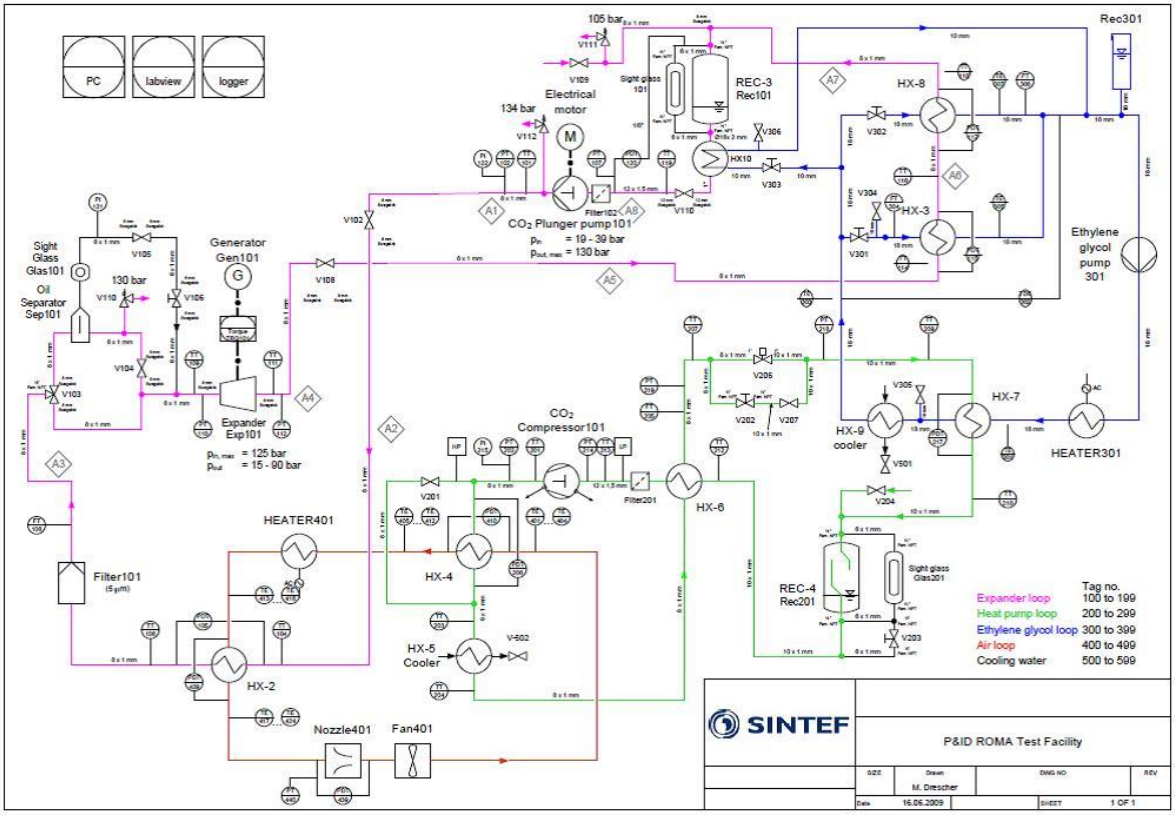

Figure 1 The detailed diagram of the test system

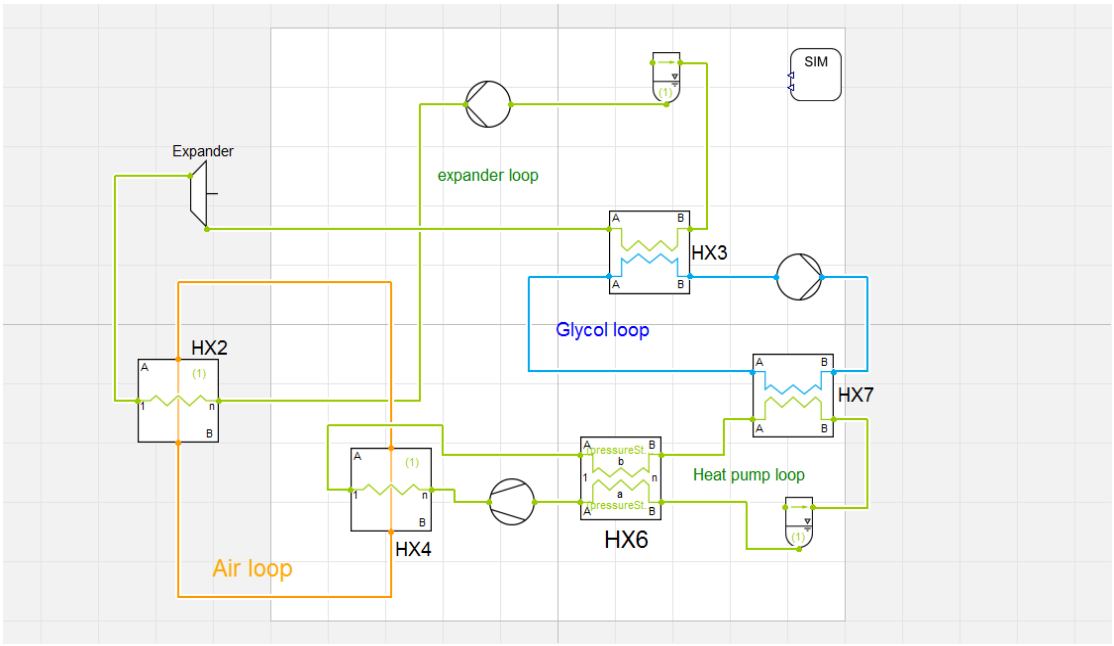

Figure 2 A simplified diagram of the test system

A. The expander loop

This is the main and central loop of the test rig. This loop is highlighted with purple lines in Figure 1, and Figure 3 is representing this loop extracted from the system, indicating the working principles of this crucial cycle of the complete system.

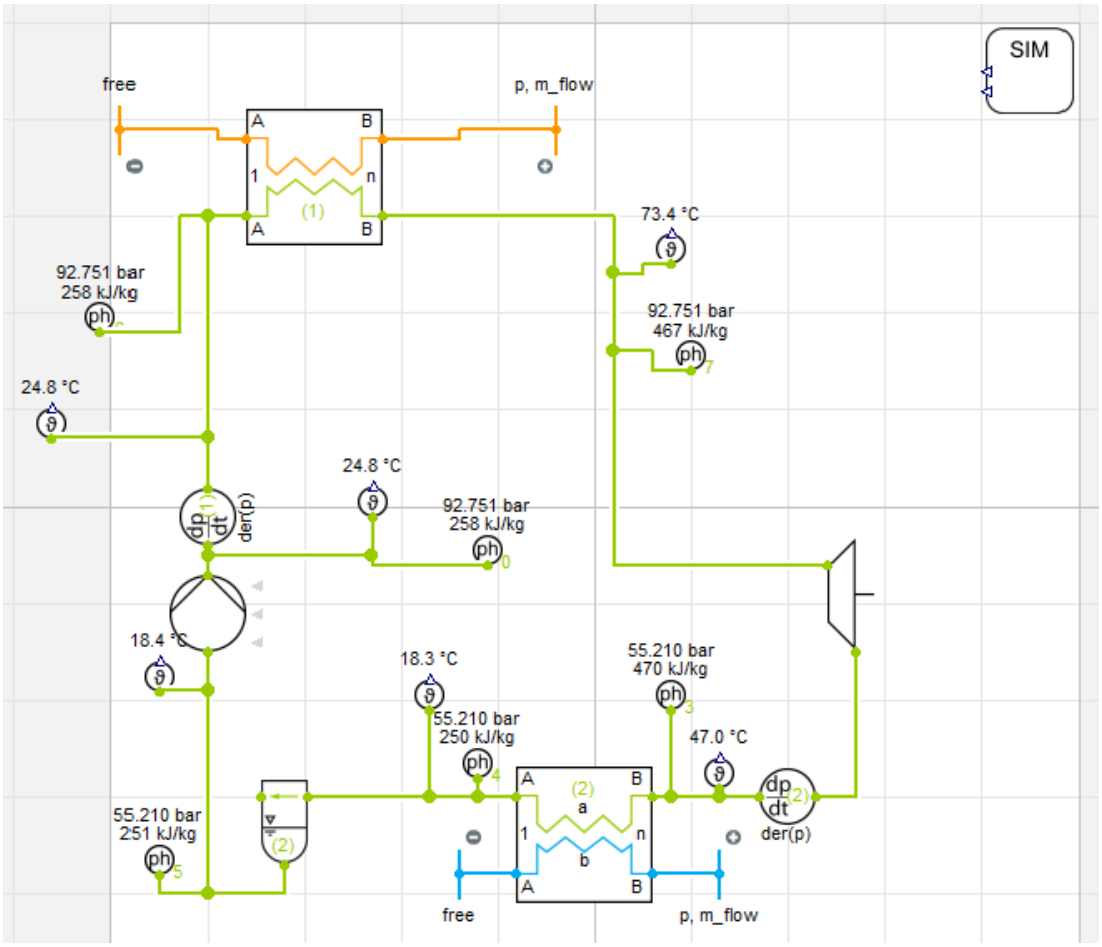

Figure 3 Explanation diagram of the expander loop

The essential component of this cycle is the expander, which provides the work output with heated working fluid of CO_2 vapor. All the other units for this cycle are selected according to the requirements of the expander, in order to maximize the work output. In the expander loop, heat input is carried out through the heat exchangers of HX-2. This cycle also changes heat with HX-3, HX-8 and HX-10, but these heat exchangers are hidden or merged in Figure 2 and Figure 3 for the sake of simplification.

Installation of a plunger pump after the condensation heat exchangers of HX-3, HX-8 and HX-10 is necessary in order to provide extra driving force to push the operation of this cycle. With consideration of preventing cavitation problem within the plunger pump, it is installed at the lowest position of the whole test rig. The place of the plunger pump guarantees the least risk of having a cavitation problem with the maximum working pressure of the working fluid. Moreover, to completely avoid cavitation, especially in the plunger pump, a liquid receiver is placed before the working fluid goes into the pump. All of these devices are designed for guaranteeing a sub-cooled fluid into the plunger pump inlet and no potential threat of having any gas phase of working fluid in the pump.

In Figure 3, the top heat exchanger is representing HX-2 in the actual test rig, connecting the expander loop to the air loop, which serves as the heating component of the working fluid and CO_2 is heated under high working pressure in this heat exchanger. Meanwhile, the bottom heat exchanger in Figure 3 is representing several merged heat exchangers in the real test rig, functioning as the cooling components after the expansion process in this loop. Further explanation of the air loop and the ethylene-glycol loop will be seen in latter parts.

The expander in this test rig is a component that converts kinetic energy of the heated working fluid into spinning movement of the generator, thus creating or providing power output. The main designed parameters of the expander are shown in Table 1. The more detailed design of this expander is classified and no more specific information can be provided here.

Table 1 Technical data chart of the expander

Parameters	Value	Unit
Maximum high pressure of the inlet	133	bar
Maximum low pressure of the outlet	90	bar
Minimum low pressure of the outlet	15	bar
Maximum temperature of the inlet	160	℃

Maximum housing temperature	80	℃
Maximum mass flow	250	kg/h
Maximum driving force	2	Nm
Rotate speed	1500-10000	rpm

This expander is specially designed for the working fluid CO_2. In order to deal with the high sensitivity for axial forces on the shaft of this component, an adjustment plate is placed to avoid potential damages. An amount of 5-10 ml of lubricating oil is injected at the inlet of the expander to smooth the operation of the expander and to seal the component. An in-built oil separator is also set in it as well.

The power generator used in this loop is a direct current dynamo machine. The data sheet of this dynamo is not acquirable. The minimum rotational speed to start the expander with a motor is 1500 rpm as in Table 1. Therefore, a direct current machine is used in order to work in a motor mode and give the rotational speed needed to start the expander. As soon as the expander has reached the rotational speed of 1500 rpm, the direct current machine can be switched from motor mode to generator mode, resulting in generating electrical power. A more simplified explanation of the direct current machine is given in Figure 4 and 5.

To make the turbine with the direct current machine function, an external battery is linked into the component, activating the direct current machine. This battery is only delivering electrical power for the direct current machine to function in the motor mode. An external device is added to prevent a potential harmful flow back current, in which case the battery might be overloaded and damaged. To convert the generated power from this loop into other forms of energy three electric lamps and a heater is installed to use the electricity provided by the generator.

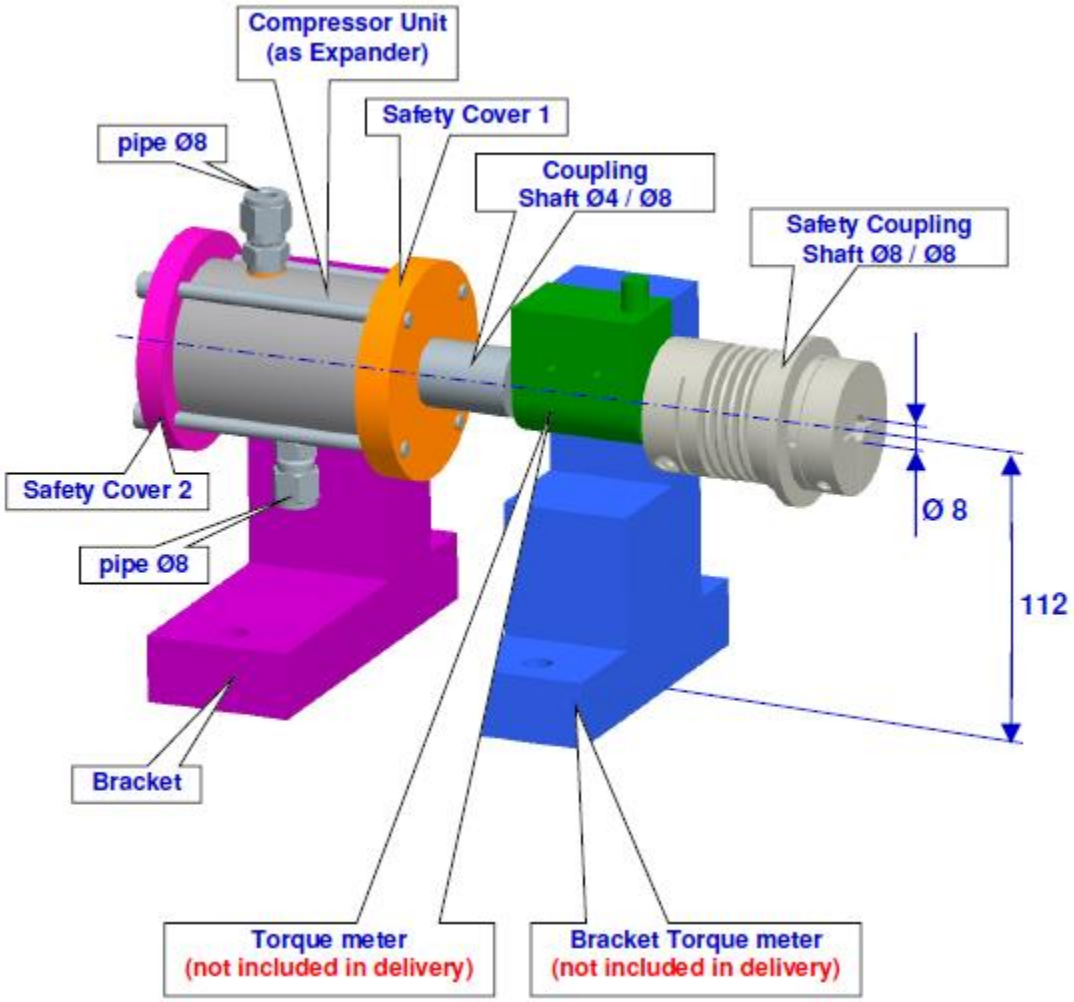

Figure 4 Expander system setting with torque meter and clutch

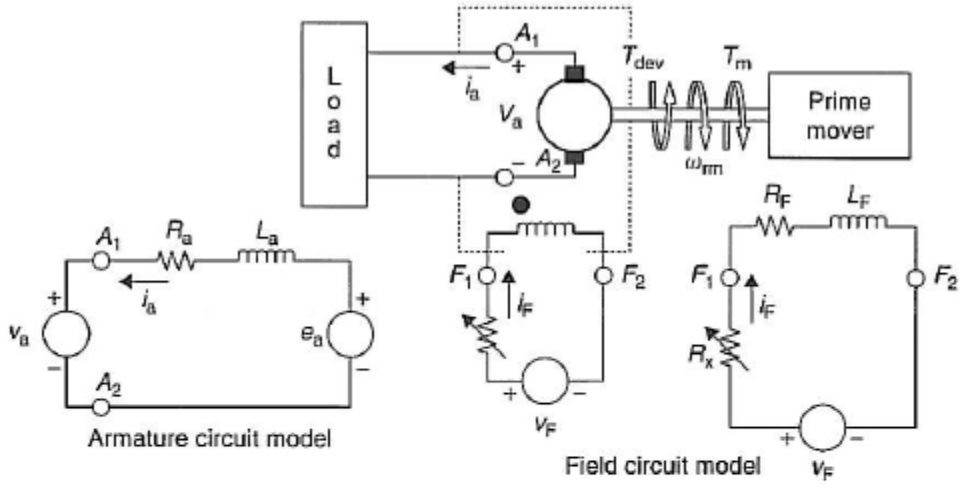

(a) Generator coordinates

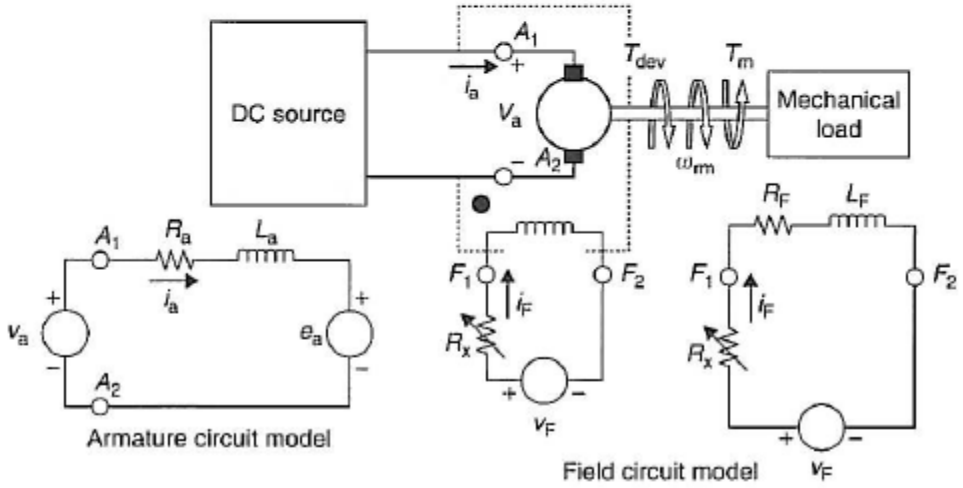

(b) Motor coordinates

Figure 5 An illustration of direct current machine in motor mode and generator mode

Figure 6 A GRUNDFOS pump in the expander loop

B. The air loop

Looking at the whole point of this designed system, the major energy input is the solar energy coming from the solar collector. However, as is mentioned above, an air loop is applied to this system playing the role of thermal energy input, thus simulating the heat source from solar energy collectors. Therefore, this loop is the driving force of the whole test rig, which is a very important part. This cycle is highlighted with red lines in Figure 1, and it is obviously seen that the major heat transfer between the

expander loop and the air loop is done in the heat exchanger of HX-2. The air loop actually utilizes a CO_2 heat pump to realize the process of heating up the air using HX-4 as condenser. Usually this cycle is in need of some supplementary heating to acquire the high temperature of the air. Therefore, the electric heater is installed to satisfy this need and provide the rest of the needed amount of heat. However, in actual operation of this air loop, the heat exchanger of HX-4 was removed in order to maintain a more stable air temperature conditions and benefit the whole tests. The recycling of the air is achieved with the help of an air fan right in front of HX-4.

C. The ethylene-glycol loop

On the low pressure side of the expander loop an ethylene-glycol loop was installed, which is highlighted with blue lines in Figure 1. At first the working fluid was pure water inside this loop, but when the tests were carried out with a relatively low condensing pressure it is of great necessity to substitute the cooling fluid with an ethylene-glycol mixture, the freezing point of which is -19.5° C. When the tests were operated with water as cooling fluid, tap water was directly used in the cooler HX-9. The main purpose of this cycle is to make sure the working fluid of CO_2 is at sub-cooled state at the expander loop, which has the below saturation temperature. This condition, as mention above in the expander loop part, is to eliminate the potential possibility to have any cavitation problem in the plunger pump. In the ethylene-glycol loop, HX-3 is a counter flow heat exchanger while HX-8 and HX-10 are tubular internal heat exchangers. The performance in cooling between these two types of heat exchangers is determined by controlling the mass flow of the cooling fluid. In other words, the distribution between these heat exchangers decides the performance. A single pump is installed to give the driving force for the cooling fluid flows.

D. The heat pump loop

For the purpose of maximizing recycled heat and achieving the best possible efficiency, this supplementary circuit of heat pump loop, which is highlighted in green lines in Figure 1, is constructed and built in the whole system. The major working components are the compressor, the condensers, the expansion device and the evaporator. These components form a complete heat pump cycle and maximize the efficiency of moving the condensation heat of the expander loop to the ethylene-glycol loop. In this heat pump loop, the heat exchanger of HX-7 functions as an evaporator, and it extracts the heat from the ethylene-glycol loop and utilizes this amount of heat to evaporate the CO_2 as the working fluid. In the heat exchanger of HX-4, the process of condensation is carried out to cool down CO_2 with air. An extra heat exchanger of HX-5 was installed to further cool down CO_2 with tap water from the water pipeline. When the heat exchanger of HX-4 was removed, the only condenser of the heat pump loop is the HX-5.

The compressor used in this heat pump loop is a semi-hermetic radial piston compressor with fixed displacement. The expansion device used in this loop is an expansion valve. An internal heat exchanger of HX-6 is set up to enhance the functioning of this heat pump, and to dehumidify the gas before entering the compressor, which otherwise would do harm to the compressor. To guarantee the gas is saturated before entering the internal heat exchanger, a liquid receiver is placed between HX-7 and HX-6. Due to the liquid receiver, changes of the working conditions at the low-pressure side are acceptable.

4.3 Measuring instruments

A. Thermocouples

The measuring thermocouples installed in this test rig had measurement limitations of up to 200° C. Such range of temperature measurements are considered necessary because at the outlet of the heater the designed temperature is close to that region. The positions of the thermocouples of the air loop are before and after HX-2, as in Figure 1. To set the thermocouples into tubes, it requires penetrating the small thin needle into the tube containing the working fluid. These thermocouples are connected to a data collector and are used to measure the temperature of working fluids including the CO_2, the ethylene-glycol water mixture and the air. These data of measurements are logged into a computer. The measuring of the thermocouples is accurate to 10^{-8}K. Most importantly, the useful thermocouples for temperature measurement were placed at the inlet and the outlet of HX-2, pump and the expander, as is shown in Figure 3.

B. Mass flow meters and pressure sensors

Besides those thermocouples, the mass flow meters and pressure sensors are also connected to the computer as well. The mass flow meters are set at the expander loop, the ethylene-glycol loop and the heat pump loop. They measure the mass flow and save data into the computer. The range of the currents of the pressure sensors and mass flow meters is 4-20 mA. And the measuring of the mass flow meters and pressure sensors is accurate to 10^{-7} kg/min and 10^{-8} bar, respectively. The monitored mass flow rate is the working fluid flow rate, which affects the performance of the system and the power output.

Figure 7 Thermal couple in the expander loop

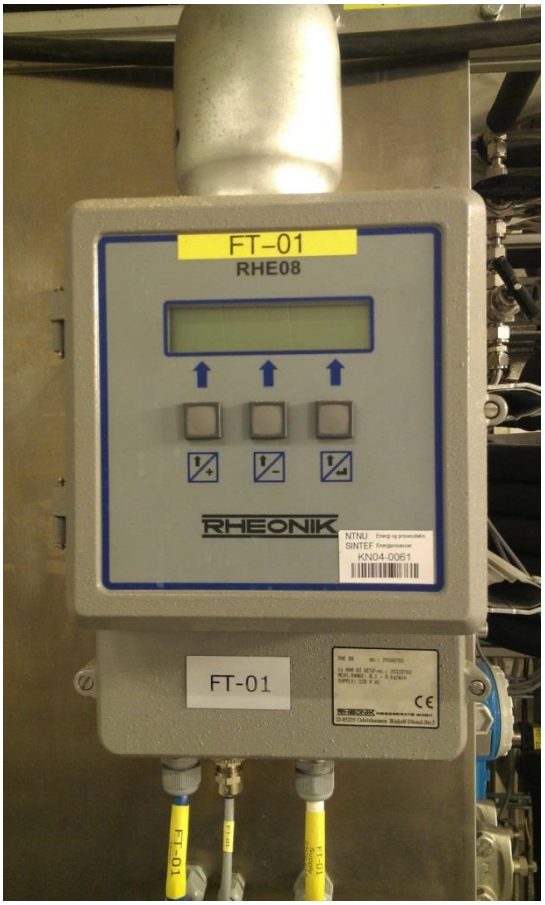

Figure 8 A RHEONIK mass flow meter in the heat pump loop

4.4 Working principles of the operation modes

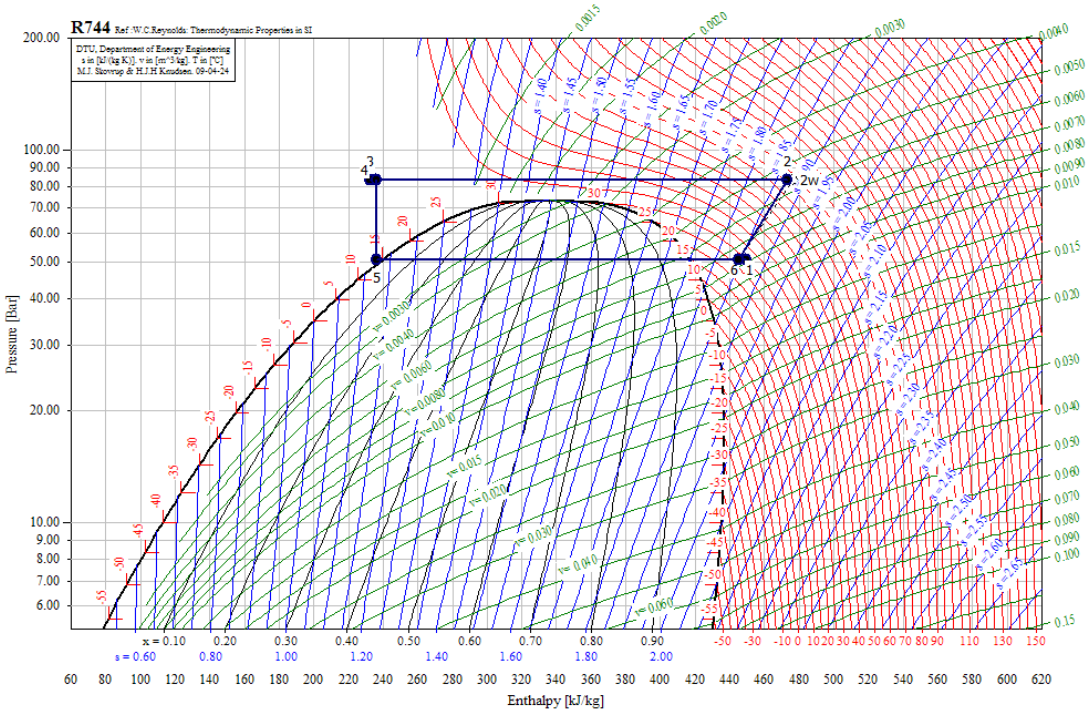

Figure 9 p-h diagram of the CO_2 in the cycle

From Figure 9 the essential processes of this system, which lies in the expander loop, can be clearly shown. CO_2 working fluid in the expander loop is heated up to super-critical state in the HX-2, the process of which is represented as state 3 to state 2 in Figure 9. At state 2, the super critical CO_2 contains a high enthalpy and is ready to go through the expander. The expansion takes place as CO_2 goes through state 2 to state 1, generating power output. Afterwards, with the help of the glycol loop, CO_2 working fluid is cooled down and goes through the two-phase state before it reaches the liquid phase, which is represented from state 1 to state 5. In order to raise the pressure of CO_2 at this stage, a pump is embedded and pumps the liquid CO_2 to state 3. In the HX-2 CO_2 is ready to be heated up again, completing a continuous cycle.

As is stated above, the crucial part of this test rig is the expander loop, for the reasons that the heat pump loop is serving as external heating equipment, simulating heat input collected from solar energy, or any other similar low grade heat source. Both the air loop and the glycol loop are acting as heat transfer equipment between high temperature end and low temperature end. The meaningful performance happens in the expander loop, providing work output and allowing us to examine the performance of super-critical CO_2 in this Rankine cycle.

4.4.1 Temperature of input heat source

From figure 7 it can be said that the temperature of input heat source plays an essential role in how the system performs. Based on the parameters and the designed working condition of components including expander, pumps and heat exchangers, the proper temperature of input heat source is between 70-100 ℃. In these actual tests, the input heat source temperature was set at 80 ℃. When operating under higher heat source temperature, such as 120-150 ℃, the system shows unstable performance attributing to higher requirement of strength of components, more severe processes of heat transfer, and less reliability of process control.

4.4.2 Pressure of expander inlet and outlet

With basic understanding of working fluid characteristics, we only need two variables of a certain state to determine all the parameters of it. In this research, for the sake of investigating working situation of supercritical CO_2, not only the temperature of CO_2 was set at proper figure, but also the pressure had to be raised to above 79.7 bar. This is to ensure that during the process of expansion and electricity generation, the CO_2 at the expander inlet was at super-critical state. Therefore, efforts of the pump in the expander loop serves as a key role in it.

4.4.3 Flow rate of CO_2

At specific working conditions, as the mass flow rate of CO_2 grows, generally the work output will grow as well. It is beyond any doubt that for enabling a higher work output, an easy way is to raise the mass flow rate of CO_2. Contradictorily, if the mass flow rate of CO_2 is raised, it will influence the heat transfer in heat exchangers. The fact is that since all the heat exchangers are already set up in the system, heat transfer process must be somehow completed in the heat exchangers to ensure the stable working state. If the mass flow rate is too high, the completeness of heat transfer in the heat exchangers might be challenged, resulting in insufficiency of both heating and cooling processes in the CO_2 loop. During the tests, the mass flow rate of CO_2 is set between 1.8 kg/min to 3.8 kg/min. This is to verify that the work output can be at a significant figure and that the heat exchanging processes can be sufficient.

4.5 Experiment results and analysis

A few series of tests were carried out to examine the performance and functions of this proposed system. From the results of these tests, the feasibility of this system is approved. All the tests were pre-set with input heat source temperature of 80 ℃. Basic analysis of the tests is presented below.

4.5.1 Power outputs of the system

Power outputs of the expander loop in the system can be determined by several variables including input heat temperature, inlet and outlet pressure of the expander, speed rate of the expander, etc. The actual tests consist of two main categories. The

first category was to fix the flow rate of working fluid, as CO_2 in this system, and change the speed rate of the expander to examine the outputs. The second category was operation with a pre-set speed rate of the expander and check out the performances under different working fluid flow rate. The work outputs of the expander can be directly measured and compared. Among the tests the highest outcome of work output was 404.34W, at the CO_2 flow rate of 3.8kg/min and the expander rate of 3500 rpm. In the meantime, the minimum work output of the tests, which was 96.528W, happened at the CO_2 flow rate of 1.8kg/min and the expander speed rate of 1500 rpm.

Table 2 Power output comparison at high flow rate

CO2 flow rate (kg/min)	Expander rotate speed (rpm)	Power output (W)
3.5	2900	295.6348067
3.5	3500	315.3359563
3.5	4500	346.0600909
3.8	2900	336.8814076
3.8	3500	371.0130681
3.8	4500	404.3446102

Table 3 Power output comparison at fixed expander rotate speed

CO2 flow rate (kg/min)	Expander rotate speed (rpm)	Power output (W)
1.8	1500	96.5275651
2	1500	105.6011862
2.5	1500	149.4952302
3	1500	178.2806743
1.8	2500	109.2533068
2	2500	107.5374258
3	2500	239.7312444
3.8	2500	300.3030858

2	3000	107.9096077
2.5	3000	231.3756113
3	3000	271.5370118
3.8	3000	336.8814076

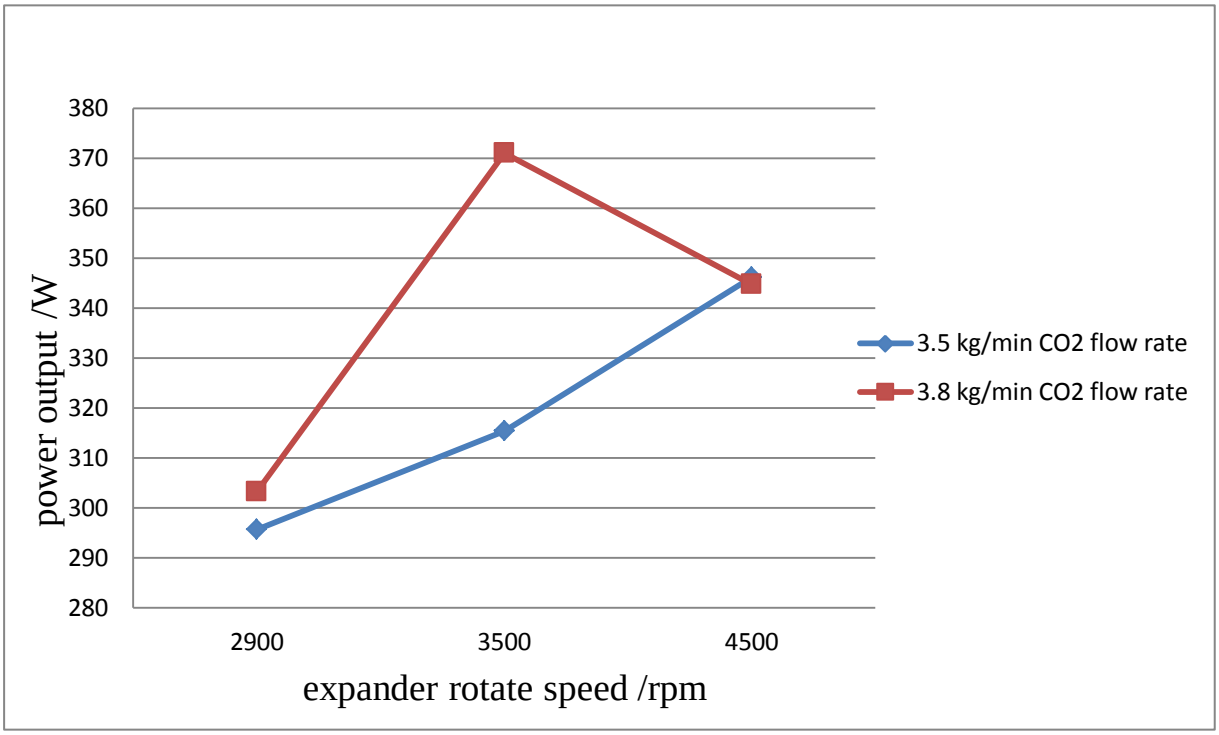

Figure 10 Power output at high CO2 flow rate

Generally the power output of the system increases under circumstances that either the CO_2 mass flow rate climbs or the expander rotate speed rate increases. The variable of CO_2 flow rate has a more significant influence on the power output in this system, which can be explained that the more CO_2 fluid going through the turbine and pushes it, naturally the work it produces will grow.

4.5.2 Turbine efficiency of the expander loop

Turbine efficiency is calculated using the Equation 2.

$$\eta_T = \frac{P_{act}}{(h_{T,in} - h_{T,out}) * \dot{m}}$$

Equation 2

η_T Turbine efficiency of the expander loop

w_{act} Actual power output of the expander [kW]

$h_{T,in}$ Enthalpy of the turbine inlet [kJ/kg]

$h_{T,out}$ Enthalpy of the turbine outlet [kJ/kg]

$\dot{m}$ Mass flow rate of CO_2 [kg/s]

With all the variety including the work output, enthalpy of turbine inlet and outlet known from the tests, turbine efficiency directly rely on CO_2 mass flow rate and features of the expander.

Judging from the experiment results, turbine efficiency varies hugely from around 47% to 82%. The testing conditions and corresponding turbine efficiency is presented in figure 9 below.

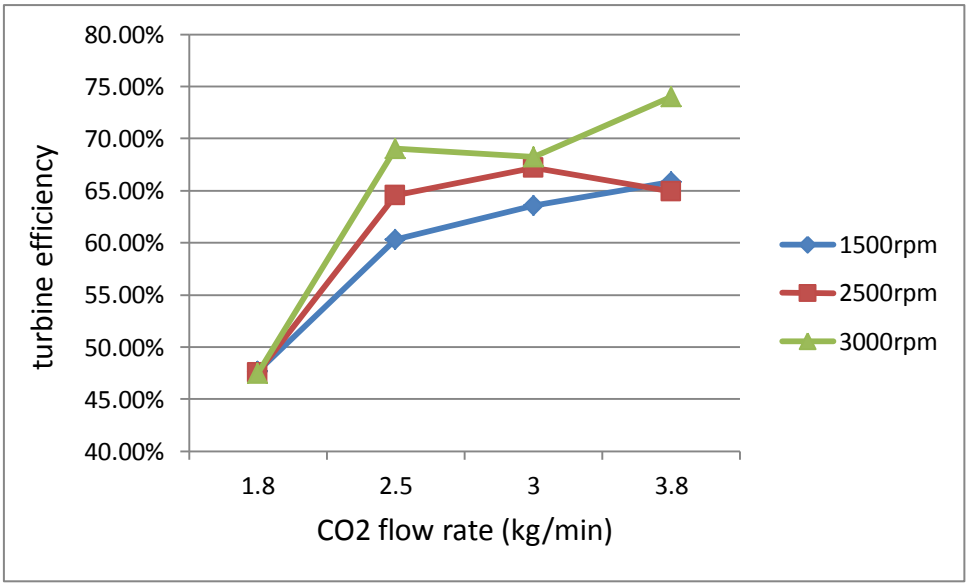

Figure 11 Turbine efficiency under different working conditions

From Figure 11 the significant increment of turbine efficiency is very apparent overall

when the expander speed rate increases. Moreover, with deeper insights, in general the turbine efficiency also relates to the flow rate of CO_2 working fluid. The tendency is quite doubtless that as CO_2 flow rate climbs from 1.8 to 3.8, turbine efficiency shifts from lower figure around 47% to a higher figure around 65%-75%. This tendency is shown regardless of the expander speed rate's variety.

Another angle to evaluate the performance and the effectiveness of the expander is the concept of isentropic efficiency. The formula used for isentropic efficiency calculation is Equation 3 below:

$$\eta_{isentropic} = \frac{h_1 - h_2}{h_1 - h_s}$$

Equation 3

$\eta_{isentropic}$ Isentropic efficiency of the expander

h_1 Actual enthalpy of the expander inlet [kJ/kg]

h_2 Actual enthalpy of the expander outlet [kJ/kg]

h_s Enthalpy of the expander outlet in isentropic expansion process [kJ/kg]

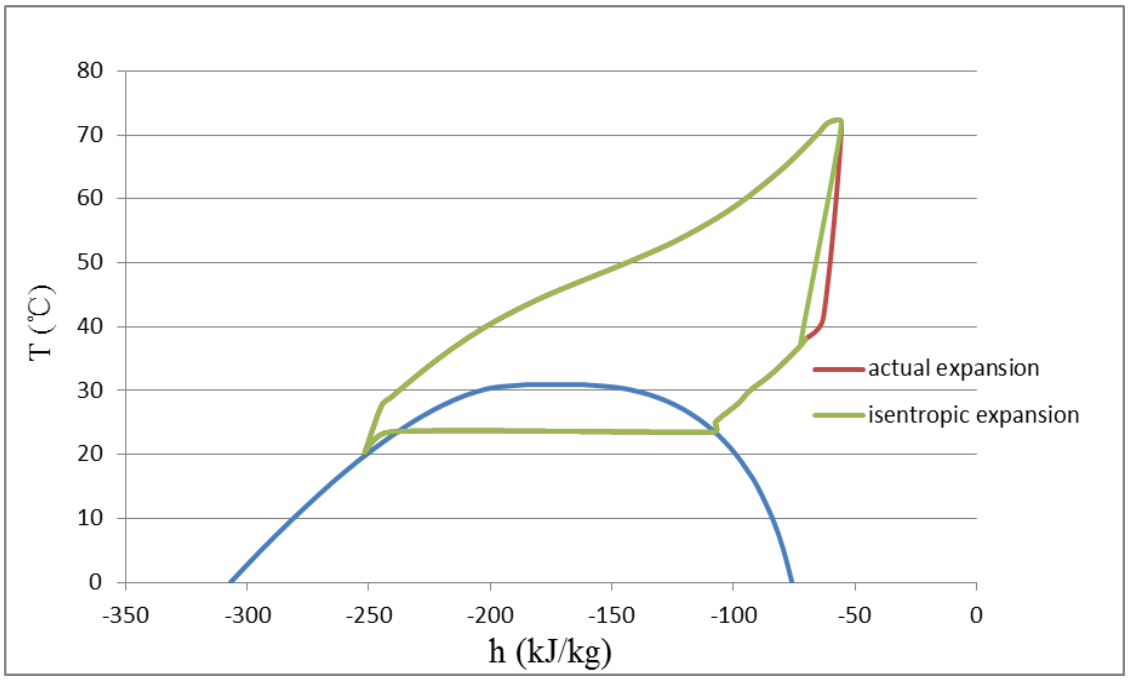

Figure 12 Diagram of actual expansion and isentropic expansion

Table 4 Comparison of isentropic efficiency under different conditions

CO2 flow rate	3.5kg/min			3.8kg/min		
expander speed (rpm)	2900	3500	4500	2900	3500	4500
isentropic efficiency	39.74%	50.36%	53.96%	38.82%	47.29%	49.23%

From Figure 12 it is clearly presented that the actual expansion process is sliding to the right side of an ideal isentropic expansion, attributing to the increment of entropy and decrement of power output. With the formula above the isentropic efficiency can be calculated based on the test results and the consequences are shown in Table 4. The doubtless tendency is that isentropic efficiency of a turbine increases as the expander speed is raised. The ideal isentropic efficiency swings around the figure of 50% at the expander speed rate of 4500 rpm.

4.5.3 Overall efficiency of the complete loop

It is of crucial importance that we calculate the overall efficiency of the complete expander loop for the sake of evaluating this system. For the reasons that this system

aims at researching the feasibility of power production under low temperature heat source such as solar energy heat sink, the critical loop of the system is the expander loop. Therefore, it is reasonable to focus on this part. Principally the overall efficiency of a system for generating electricity from heat source is defined as the ratio of actual work output and the heat input. To present in terms of a formula it is as below:

$$\eta_{overall} = \frac{P_{act}}{Q}$$

Equation 4

$\eta_{overall}$ Overall efficiency of the expander loop

P_{act} Actual power output of the expander [kW]

Q Heat absorbed in the HX-2 of the expander loop [kJ]

With the results of the tests, the overall efficiency is calculated under different working conditions.

The first result we can get is as the expander speed rate increases, the overall efficiency rises as well generally. Two sets of experiment data were chosen to support this result, as it is easily concluded from Figure 13.

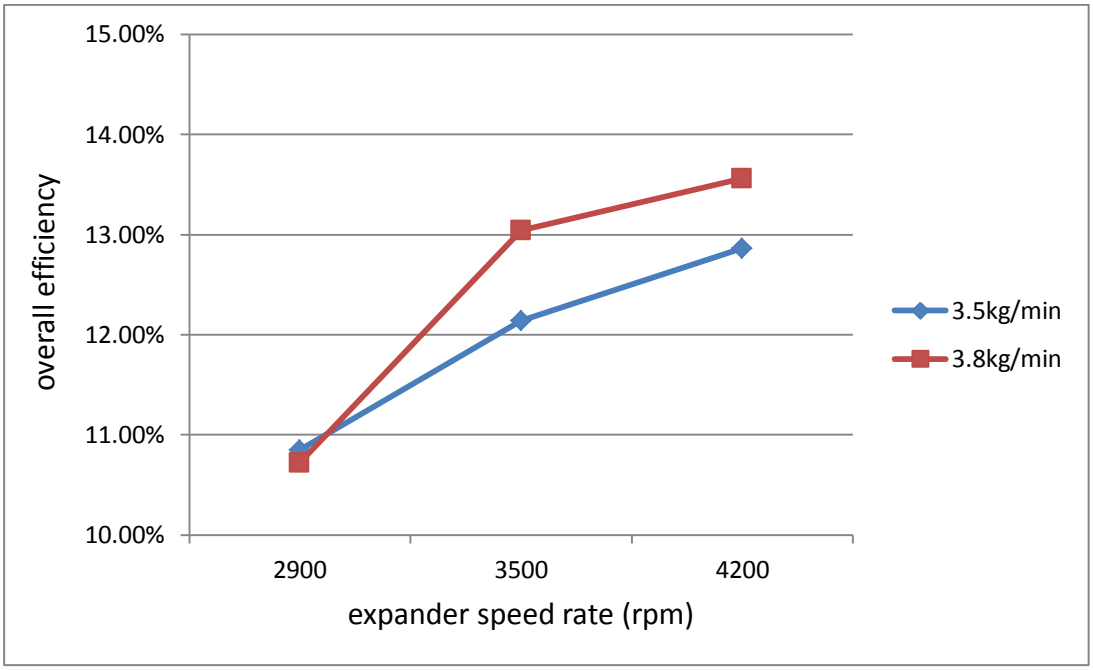

Figure 13 Relation between expander speed rate and overall efficiency

The second result comes from comparison among different CO_2 mass flow rate, under various expander speed rate. The tendency is clear that with higher CO_2 flow rate comes higher overall efficiency, but the efficiency climbs very slowly when the CO_2 flow rate reaches a certain figure and keeps climbing. The diagrams of this comparison are presented in Figure 14-16 below.

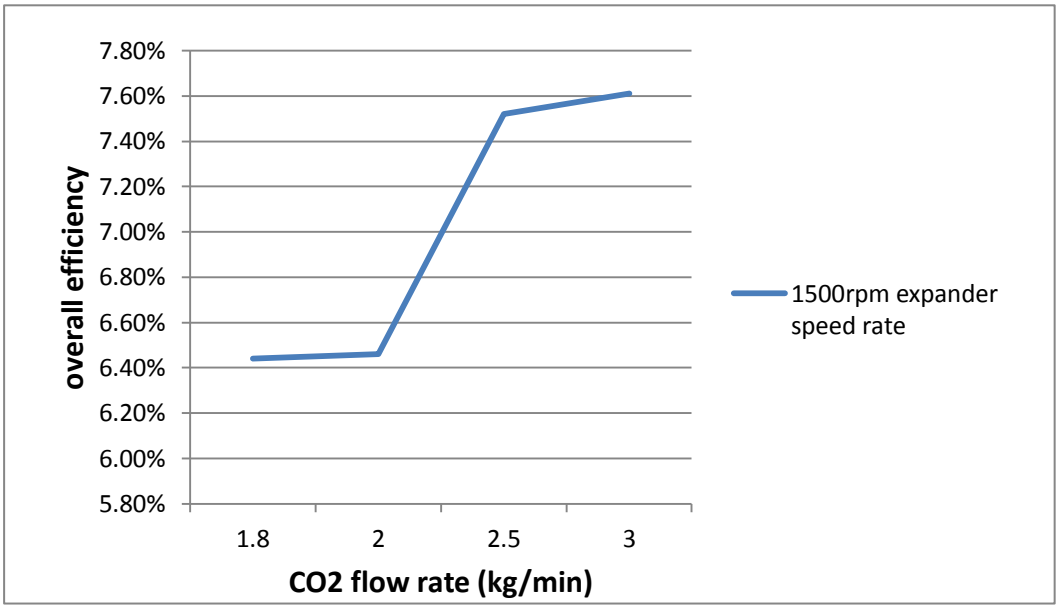

Figure 14 Overall efficiency at 1500 rpm expander speed rate

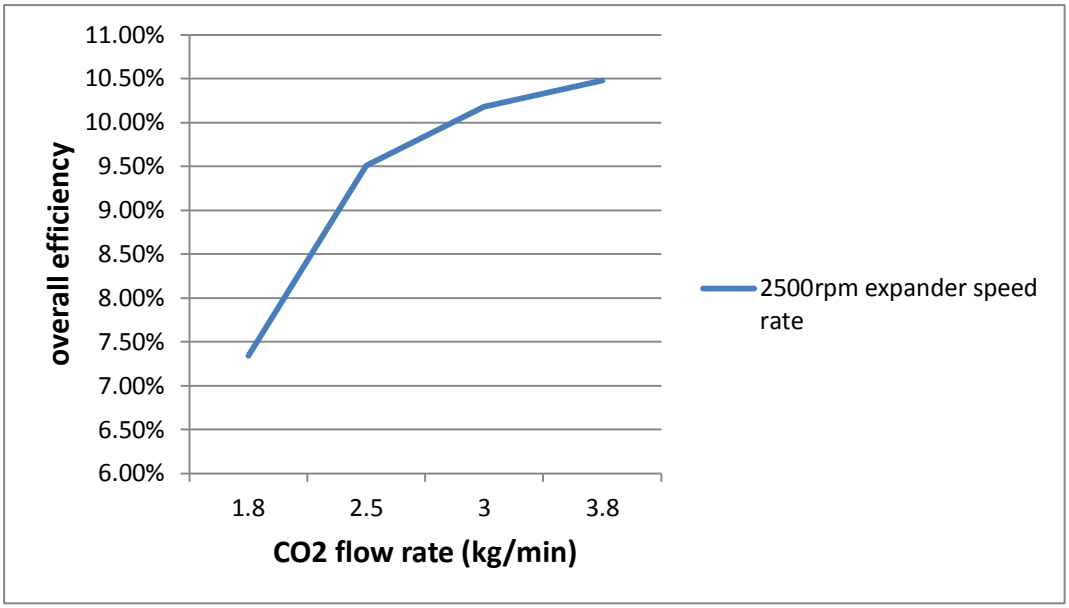

Figure 15 Overall efficiency at 2500 rpm expander speed rate

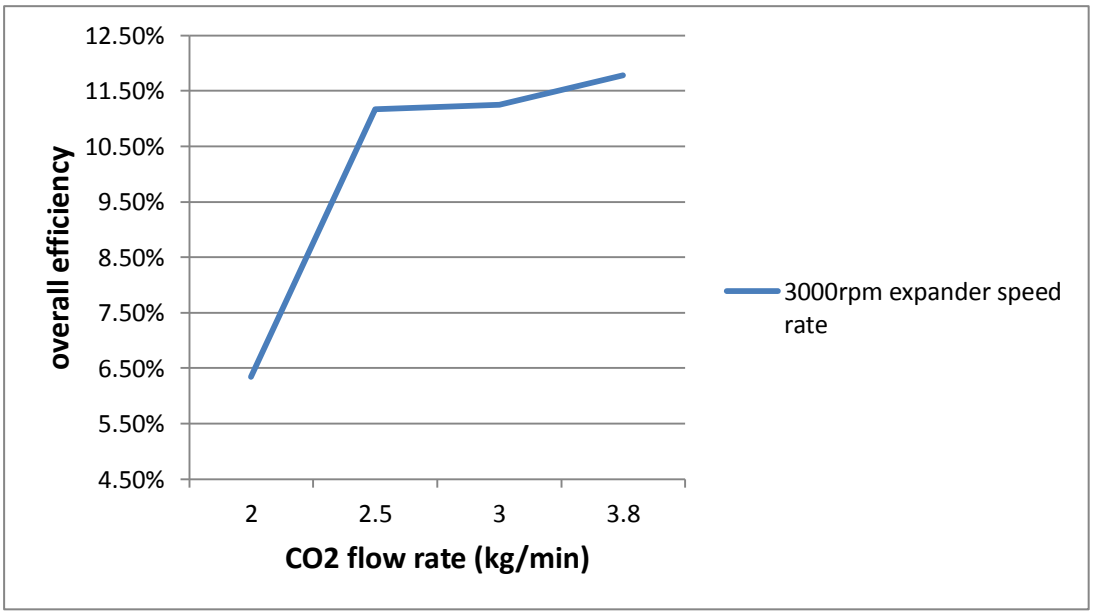

Figure 16 Overall efficiency at 3000 rpm expander speed rate

4.6 Evaluation of the experiments

From the perspective of effect, these experiments offered an abundant series of proof for the feasibility of power generation of this Rankine cycle utilizing CO_2 as working fluid and low grade heat source, presumably solar energy input. As the simulation of

heat input was set at a temperature of 80 ℃, the results are plain and suitable for analysis. Furthermore, in the comparison of testing results and the analysis, essential features or variables including expander speed rate and mass flow rate of CO_2 are examined and quantified. It can be safely concluded that the primary feasibility of the system is verified with the results.

Another critical analysis was that through calculation, the turbine efficiency and overall efficiency of the expander loop were acquired. The turbine efficiency varies significantly throughout the tests, probably due to the potential incapability for the expander to work out the super-critical CO_2. After all, the expander that was abducted in the test rig was not specially designed to deal with super-critical CO_2 in this case. Further details for turbine efficiency analysis are remained to be examined for future study and research. On the other hand, the overall efficiency was fluctuating between 0.06-0.13, which is an optimistic result. This overall efficiency neglected the irreversibility and dissolving effect of the heat inputting process because it was calculated using entropy increment between the inlet and the outlet of HX-2. Therefore, the overall efficiency will drop a little if the dissolving effect was taken into consideration. However, the results of the tests are still promising and reveal a good potential for future application.

4.7 Limits of the experiments

As for the limitation of the experiments and analysis, it has to be acknowledged that if the heat source temperature is raised higher, it will hugely improve the thermodynamic cycle in principles. All the tests were carried out under the heat input temperature of 80 ℃. But higher temperature of heat input will create bigger gap between the inlet and the outlet of HX-2, thus making a bigger gap as well between the inlet and the outlet of expander, bringing certainly a better work output.

Unfortunately, the test rig does not allow such higher temperature of heat input. As a compensating solution, a computational model was established and verified to this test rig. The performance of the computational model will be analyzed within simulation. After creating a model that is close enough to the real system, some off-design can be executed to reveal some untested results by raising the heat input temperature in the modeling condition.

5. Modelling and validation

To better analyze this system, it is of significant importance to establish a computational model in order to run a simulation. Therefore, a model was created in this research work using Modelica in Dymola platform for optimization.

5.1 Establishment of the model

Firstly, a draft model was established to simulate the whole system in functioning. Without jeopardizing any operational principles and core equipment, the system was to some extends simplified, thus focusing the computational resource on the essential modules. The diagram of simulated model is shown in Figure 17.

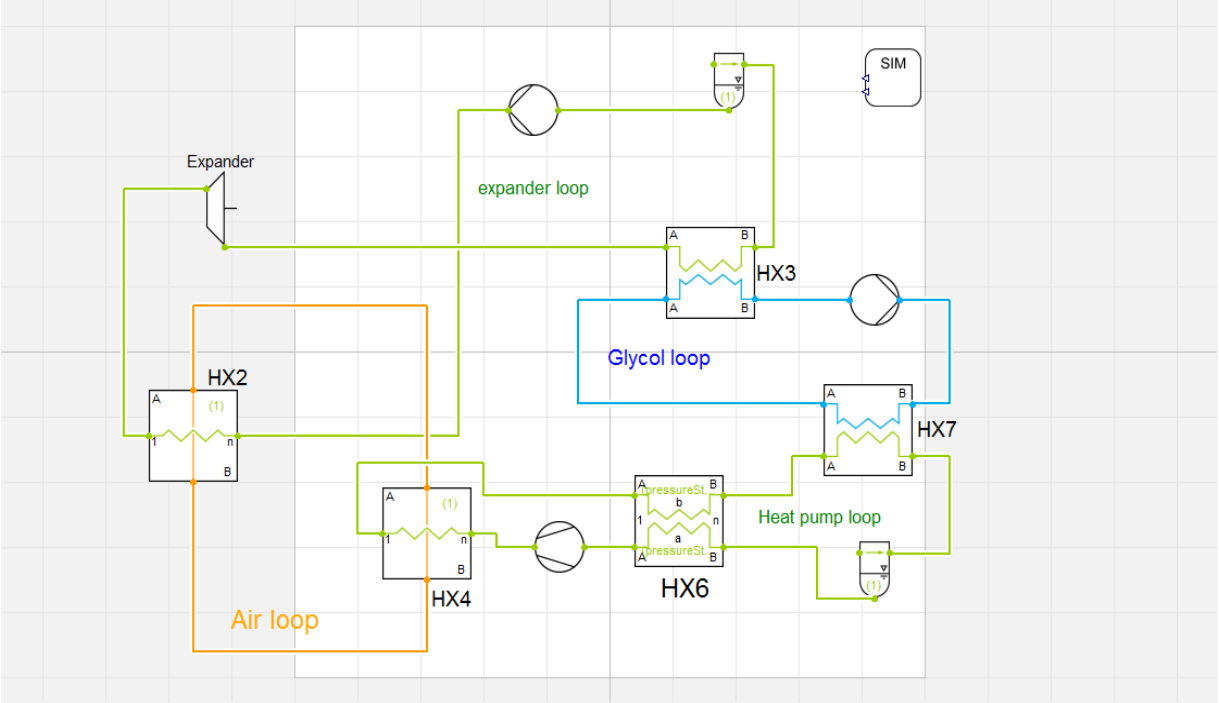

Figure 17 Simulation model diagram of the test system in Dymola

From Figure 17 it can be seen that all the four loops constructing the whole system were included in the model. Both the expander loop and the heat pump loop are colored green because they were both filled with CO_2 as their working fluid. As is mentioned above, the expander loop is the most essential loop in this system and in this simplified model it contains the heating process of CO_2 in HX-2, which is the key process of heat input. Air was heated due to the heat pump loop and transfer heat into CO_2 to convert it to super critical phase and function the expander loop. After CO_2 finished the expansion process in the expander, it was cooled down to liquid phase with the gas cooler of HX-3. In the real system, the cooling down process took place in both HX-3 and HX-8. However, in the simulation model it is of no harm to simplify this process into one gas cooler. The heat pump loop generated a high temperature CO_2 in the HX-4 and the in operation this heat was transferred to the air side in HX-4. The air loop plays a role as a media to carry the energy between the heat pump loop and the expander loop.

5.2 Validation of the model

After the simulation model is primarily established, a series of optimization progress must be done for making the computational model as close to the real system as possible.

Firstly, the detailed information of all the heat exchangers was acquired with the help of SINTEF staff. In the simulation model, the specific parameters of all those heat exchangers should be modified and adjusted to the real ones. For the essential expander loop, the information of HX-2, a fin-and-tube heat exchanger, is listed in Table 5 below.

Table 5 Key Data of HX-2

core length	**finned tube length**	**fin type**
0.615m	0.6m	corrugated
fin material	**tube material**	**tube arrangement**
aluminum	copper	staggered up
tube diameters	**fin spacing**	**tube inner area**
7.20/5.80mm	2.50mm	0.966 ㎡
number of vertical tubes	**number of horizontal tubes**	**air side area**
6	14	22.82 ㎡

With the real details of HX-2 acquired and embedded to the computational model, the physical model of HX-2 is established from Dymola's TIL module. HX-2 is a fin-and-tube heat exchanger, with numbers of cells equal to 10. The physical model can be shown in Figure 18 below.

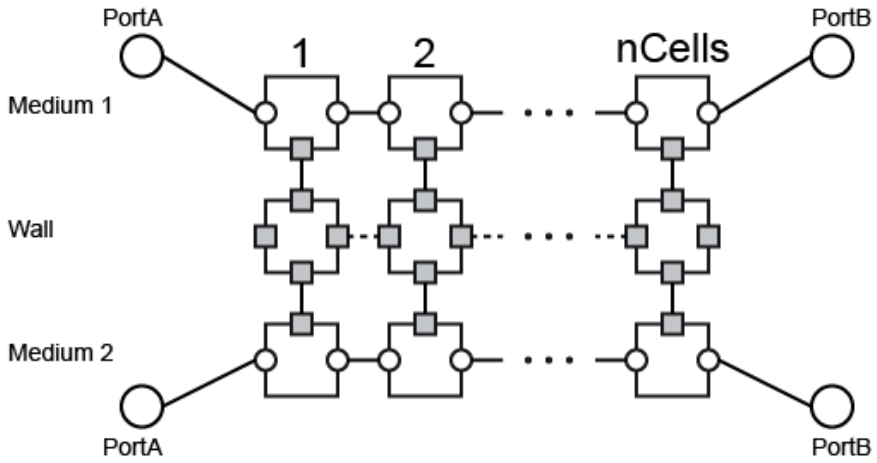

Figure 18 The model of heat exchangers used in simulation calculation

The basic conduction heat transfer principle formula is Equation 5.

$$\phi = \mathrm{kA}(t_{f_1} - t_{f_2})$$

Equation 5

ϕ Amount of heat transfer between two units [kJ]

A Area of heat transfer surface [m^2]

k Coefficient of heat transfer [kW/($m^2 * K$)]

t_{f_1} Temperature of medium 1 [℃]

t_{f_2} Temperature of medium 2 [℃]

The input data of HX-2 is Medium 1 temperature at Port A and Medium 2 temperature at Port B of this model, representing the temperature figure received from data tunnel. In Figure 18 the thermal heat resistance is presented. The adjusted formula for calculation of each cell is Equation 6.

$$\phi = \frac{t_{f_1} - t_{f_2}}{\frac{1}{h_i A_i} + \frac{\delta}{\lambda A_i} + \frac{1}{h_o \eta_o A_o}}$$

Equation 6

ϕ Amount of heat transfer between two units [kJ]

t_{f_1} Temperature of medium 1 [℃]

t_{f_2} Temperature of medium 2 [℃]

h_i Coefficient of convection heat transfer in the inside surface [kW/$(m^2 * K)$]

A_i Area of the inside surface [m^2]

δ Thickness of the heat transfer pipe [m]

λ Coefficient of conduction heat transfer in the wall [kW/$(m^2 * K)$]

h_o Coefficient of convection heat transfer in the outside surface [kW/$(m^2 * K)$]

η_o Overall fin surface efficiency

A_o Area of the outside surface [m^2]

Using iteration for solving this series of linear equations on each cell, the export data of HX-2 is Medium 1 temperature at Port B and medium 2 temperature at Port A.

Similarly, such adjustments were also made for HX-3, HX-4, HX-6, and HX-7. The information of HX-3, which served as the condenser for the expander loop, is shown in Table 6. It is a 25-plate-one-pass model, and has been insulated with 2cm thick isolation.

Table 6 tested information of HX-3

	side 1	**side 2**
port diameter	24.0mm	24.0mm
number of channels	9	10
number of plates	20	

Since the glycol loop serves for cooling CO_2 of the expander loop in HX-3 and

providing an evaporator/heat sink for the heat pump loop, it carries heat between HX-3 and HX-7. The HX-7 is a plate heat exchanger delivered by SWEP. It is a 30-plate-1-pass model.

The heat pump loop was equipped with an internal heat exchanger of HX-6, designed by SINTEF.

Table 7 Key data of HX-6

	inner diameter	outer diameter	material
high pressure tube	6mm	8mm	copper
low pressure tube	15mm	17mm	stainless steel
tube length		2m	

As for HX-4, a fin and tube heat exchanger plays a role of conveying the heat to supply the heat source, the information of which is listed in Table 8. The design of it was based on simulations with the in house design tool HXsim.

Table 8 information of HX-4

core length	**finned tube length**	**fin type**
0.815m	0.6m	corrugated
fin material	tube material	tube arrangement
aluminum	copper	staggered up
tube diameters	fin spacing	tube inner area
7.20/5.80mm	2mm	1.24 ㎡
number of vertical tubes	number of horizontal tubes	air side area
6	18	36.1 ㎡

After all the heat exchangers are properly adjusted to the real parameters, further steps of optimization need to be executed.

The expander model defines a pressure decrease, a mass flow rate or a volume flow rate. One of the variables can be a fixed value or set by a changing input from outside. Also the expander's outlet enthalpy or temperature is a fixed user-defined value. In

this model, the mass flow rate is determined by parameter input, and the discharge temperature is user-fixed in order to define the output pressure. With these parameters and a given expander efficiency, the work output is therefore calculated based on the Equation 7 below.

$$P_{out} = \eta_{exp} * \dot{m} * (h_{in} - h_{out})$$

Equation 7

P_{out} Power output of the expander [W]

η_{exp} Efficiency of the expander

$\dot{m}$ Mass flow rate of CO_2 [kg/s]

h_{in} Entropy of the expander inlet [kJ/kg]

h_{out} Entropy of the expander outlet [kJ/kg]

The pump model calculation is also based on mass balance equation and energy balance equation. Being part of a complete loop, the mass flow rate is unified and preset as well. The pump efficiency is preset at 0.4, according to the average results of the real tests.

As is analyzed above, the work output is determined by many factors, including input temperature of heat source, CO_2 working fluid flow rate, pressure raise brought by the pump in the expander loop, cooling effect of the glycol loop, etc. Generally speaking, it is impossible to 100% simulate the real situation due to the inadequate information of all components of this quite huge system. As far as current research, the exact principles and exact explicit heat transfer calculation in real complex system are not revealed yet. In most situations, including computational models, only experimental equations are applied with certain coefficients. To determine these coefficients in heat transfer, a series of modification and comparison must be executed in optimizing the simulation model in Dymola. With a set of most suitable coefficients used in the running of simulation model and the actual tested condition parameters

input, the outcomes of this simulation model were approaching quite closely to the results of the test rig.

At the CO_2 flow rate of 2kg/min, input heat source temperature set at 80℃, inlet pressure of the expander at 82.673 bar, the diagram of the simulation results in the expander is shown in Figure 19 below.

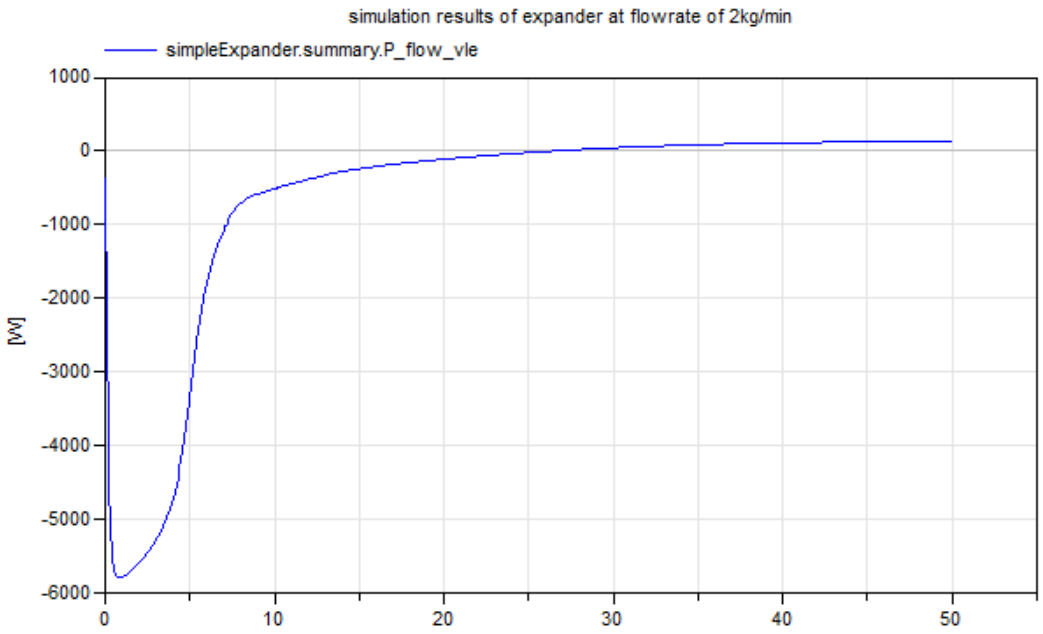

Figure 19 Diagram of simulation expander at flow rate of 2kg/min

In the simulation, the expander quickly reaches a stable state after starting operation. The stable state is obtained within 15 milliseconds. The stable work output of this simulation expander is acquired in simulation as 132.90W. To compare, the actual test result of the work output at the same condition setting is 156.464W.

At the CO_2 flow rate of 3kg/min, input heat temperature still set at 80 ℃, and the inlet pressure of the expander at 100.88 bar, the diagram of the simulation is shown in Figure 20 below.

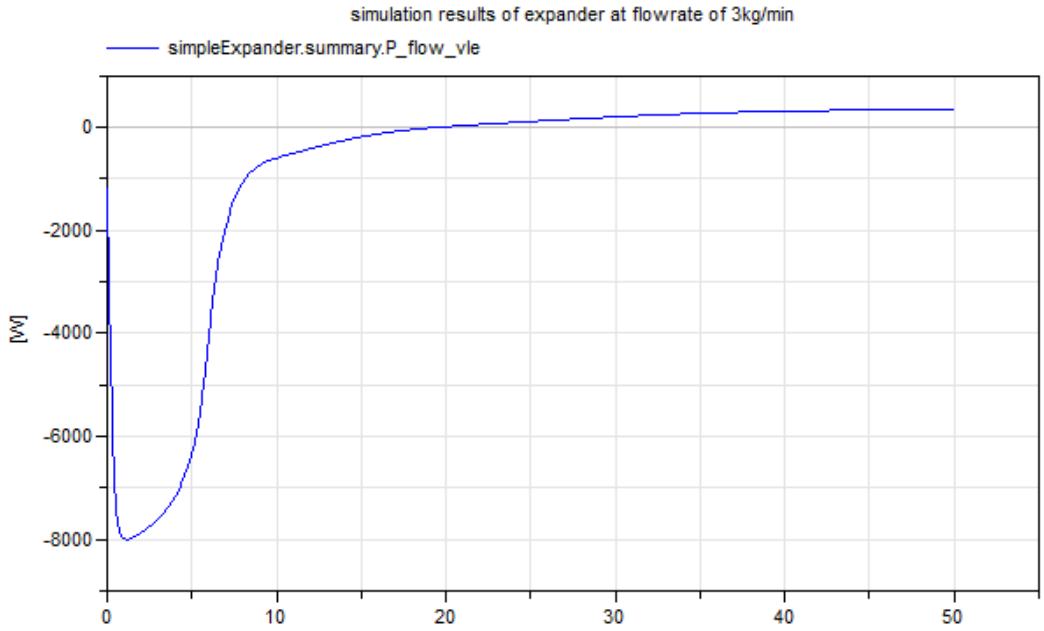

Figure 20 diagram of simulation expander at flow rate of 3kg/min

As before, the stable working state was also acquired quickly within 15 milliseconds. At these condition settings, the simulation work output by the computational model is 304.92W, while the actual test result of the work output is 257.48W.

With other series of settings, the simulation model all performed closely to the real situation as well. Basically speaking, the simulation results indicated that the difference between the computational model and the actual system is small enough to be accepted.

5.3 Extensions of the experimental conditions

As is stated above, the computational model in Dymola was established and verified as close to reality as acceptable. The major purpose of this type of model was to get over all the actual restraints and extend the working conditions to further situations. As explained in Chapter 4, the tests were all conducted under a pre-set heat source temperature of 80 ℃. The feasibility of successful operation was already testified and

proved through the testing section. However, in the primary analysis it is obviously agreed that if the input heat source temperature can be raised higher, the work output will be significantly improved. To examine this feasibility, the working condition was extended in the computational model. The main adjustment was to raise the input heat temperature to a higher figure. When the input temperature was raised, the working fluid of CO_2 matched to a higher temperature state, containing a higher entropy value. The extended working cycle is simulated in Figure 21 below:

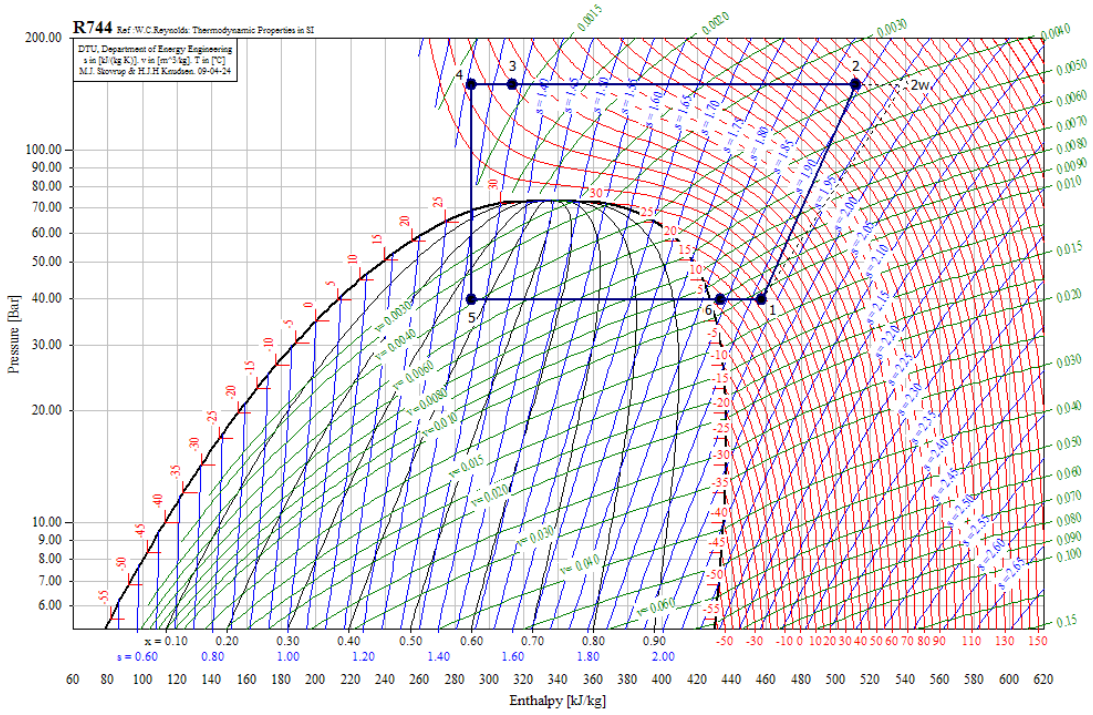

Figure 21 P-h diagram of CO_2 in extended working condition simulation

The working condition, specified as input heat source temperature was set to as high as 200 ℃, the result was that the work output climbed from around 200-300 W to 7000 W. However, there are a series of other factors influencing this result. As the input heat source temperature was raised to a higher level, the discharged temperature will also climb, leading to a situation where more cooling capacity is required in the gas cooler of the glycol loop. If the cooling capacity in HX-3 didn't get strengthened by lowering the temperature or raising the mass flow rate of cooling liquid, the state

of CO_2 after gas cooler HX-3 will be a mixture of gas state and liquid state, not sufficiently cooled down to be completely liquefied. This will severely influence the performance and cause irreversible damage of the components.

Although the results of the computational model and its simulation are too optimistic by estimation, it still shows a huge potential in this system for power generation when a higher temperature heat source can be acquired.

6. Analysis and Conclusions

6.1 Entropy analysis

For a closed system, the entropy is defined as in Equation 8.

$$\delta S_g = \mathrm{dS} - \mathrm{d}S_f$$

Equation 8

S_g is entropy generation, which can measure the irreversibility of processes. In this equation, $\mathrm{d}S_f$ is entropy flow, which is defined as Equation 9.

$$\mathrm{d}S_f = \frac{\delta Q}{T_r}$$

Equation 9

δQ Heat absorbed [J]

T_r Ambient temperature [℃]

In a heating process such as what happens for CO_2 working fluid in HX-2, CO_2 absorbs a certain amount of heat through an irreversible process. Therefore, entropy generation can be used to describe how much the irreversibility is in these processes.

With higher entropy generation comes more irreversibility and more wasted energy in the heat transfer processes.

In this part of analysis, some sets of contrary will be presented to indicate the entropy generation calculated with the equations above.

6.1.1 At fixed flow rate

Based on the equation of entropy generation, as Equation 10 below, the entropy generation S_g of each component and the whole expander loop is listed in Table 9 and Table 10 below. The input heat source temperature is 80 ℃ for both tables.

$$\delta S_g = \mathrm{dS} - (\frac{\delta Q}{T_r})$$

Equation 10

δQ Heat absorbed [J]

T_r Ambient temperature [℃]

Table 9 S_g (kJ/kg*K) of the expander loop at 3.5kg/min

expander speed rate	HX-2	turbine	HX-3	pump	sum
2900rpm	0.097456	0.047564	-0.08905	-0.01456	0.04141
3500rpm	0.062272	0.04183	-0.08993	-0.01216	0.002012
4200rpm	0.063093	0.041246	-0.0919	-0.01216	0.000279

Table 10 S_g (kJ/kg*K) of the expander loop at 3.8kg/min

expander speed rate	HX-2	turbine	HX-3	pump	sum
2900rpm	0.079665	0.045818	-0.10823	-0.01462	0.002633
3500rpm	0.062884	0.04483	-0.08986	-0.01528	0.002574
4500rpm	0.057737	0.04213	-0.08516	-0.01273	0.001977

From the calculation of entropy generation, it appears that the higher expander speed rate is adopted, the less irreversibility of the system can be achieved. The main reason for this phenomenon can be laid in that high expander speed brings more efficient performance in the turbine, thus reducing the negative influence of friction loss and wasted energy.

6.1.2 At fixed expander speed rate

The same method of analysis is also applied for fixed expander speed rate. In order to detect the tendency of entropy generation in increasing expander speed rate, contrary of entropy generation and irreversibility is revealed in the tables 11-13.

Table 11 S_g (kJ/kg*K) of the expander loop at 1500 rpm expander speed

Flow rate	HX-2	Turbine	HX-3	pump	sum
1.8kg/min	0.085292	0.040263	-0.1088	-0.00678	0.009975
2kg/min	0.079722	0.03928	-0.10528	-0.00748	0.006242
2.5kg/min	0.066949	0.04828	-0.09901	-0.01008	0.006139
3kg/min	0.055776	0.053864	-0.0914	-0.01473	0.00351

Table 12 S_g (kJ/kg*K) of the expander loop at 2500 rpm expander speed

Flow rate	HX-2	Turbine	HX-3	pump	sum
1.8kg/min	0.094895	0.031096	-0.11178	-0.00623	0.007981
2.5kg/min	0.070935	0.041397	-0.09806	-0.00961	0.004662
3.0kg/min	0.063297	0.046963	-0.09432	-0.01101	0.00493
3.8kg/min	0.050603	0.051246	-0.08486	-0.01626	0.000729

Table 13 S_g (kJ/kg*K) of the expander loop at 3000 rpm expander speed

Flow rate	HX-2	Turbine	HX-3	pump	sum
2.0kg/min	0.087875	0.02998	-0.10497	-0.00622	0.006665
2.5kg/min	0.072501	0.04039	-0.09691	-0.00961	0.006371
3.0kg/min	0.065516	0.04438	-0.09289	-0.0119	0.005106
3.8kg/min	0.05147	0.049397	-0.08228	-0.01571	0.002877

It can be concluded that generally with higher flow rate of working fluid comes lower

entropy generation in the expander loop overall, which by estimation is resulted from more efficient heat transfer processes in heat exchangers under higher flow rate of working fluid. According to heat transfer principles, higher fluid speed can generally enhance the efficiency of conduction, thus giving better performances in reducing entropy generation. However, flow rate can't be unlimitedly increased due to limitations of equipment, such as pump capacity and turbine capacity. From the testing section, the most beneficial flow rate is 3.5-3.8kg/min of CO_2 in the expander loop considering the irreversibility of system.

6.2 Exergy analysis

The most basic principle of exergy analysis is the limits of heat converting to work. When the ambient temperature is T_0, the maximum work output from a heat source with temperature T is calculated with Equation 11.

$$w_{max} = (1 - \frac{T_0}{T})\mathrm{q}$$

Equation 11

w_{max} Maximum work output [J]

T_0 Ambient temperature [℃]

T Temperature of heat source [℃]

So in a certain thermal loop, the exergy of working fluid after absorbing heat is determined in Equation 12.

$$e_{x,Q} = \int_1^2 \delta q - T_0 \int_1^2 \frac{\delta q}{T}$$

Equation 12

$e_{x,Q}$ Exergy of working fluid [J/kg]

T_0 Ambient temperature [℃]

T Temperature of heat source [℃]

With the definition of entropy, the equation becomes Equation 13.

$$e_{x,Q} = \mathrm{q} - T_0 \Delta S$$

Equation 13

$e_{x,Q}$ Exergy of working fluid [J/kg]

q Heat absorbed[J/kg]

T_0 Ambient temperature [℃]

ΔS Entropy increment [J/kg*K]

For the exergy loss in a closed cycle's irreversible processes, entropy function can serve for the solution. From the insight of internal connection between entropy increment and exergy loss in a closed isolated cycle, they both result from irreversibility of the processes, thus making it reasonable to calculate exergy loss with this equation 14.

$$E_{X,l} = T_0 S_g$$

Equation 14

$E_{X,l}$ Exergy loss [J/kg]

T_0 Ambient temperature [℃]

S_g Entropy generation [J/kg*K]

Based on this exergy loss equation, it is quite plain to calculate the exergy loss of the expander loop in the model of simulation. The ambient temperature is 15℃, and the

entropy generation S_g was already calculated in **section 6.1**. The results are presented in tables 14-18.

6.2.1 At fixed expander speed rate

Table 14 Exergy loss (kJ/kg) at 1500 rpm of the expander loop

Flow rate	HX-2	Turbine	HX-3	pump	sum
1.8kg/min	24.564096	11.595744	-31.3344	-1.95264	2.8728
2.0kg/min	19.281312	13.90464	-28.51488	-2.90304	1.768032
2.5kg/min	22.959936	11.31264	-30.32064	-2.15424	1.797696
3.0kg/min	16.063488	15.512832	-26.3232	-4.24224	1.01088

Table 15 Exergy loss (kJ/kg) at 2500 rpm of the expander loop

Flow rate	HX-2	turbine	HX-3	pump	sum
1.8kgmin	27.32976	8.955648	-32.1926	-1.79424	2.298528
2.5kgmin	20.42928	11.92234	-28.2413	-2.76768	1.342656
3.0kgmin	18.22954	13.52534	-27.1642	-3.17088	1.41984
3.8kgmin	14.57366	14.75885	-24.4397	-4.68288	0.209952

Table 16 Exergy loss (kJ/kg) at 3000 rpm of the expander loop

Flow rate	HX-2	turbine	HX-3	pump	sum
2.0kg/min	25.308	8.63424	-30.23136	-1.79136	1.91952
2.5kg/min	20.880288	11.63232	-27.91008	-2.76768	1.834848
3.0kg/min	18.868608	12.78144	-26.75232	-3.4272	1.470528
3.8kg/min	14.82336	14.226336	-23.69664	-4.52448	0.828576

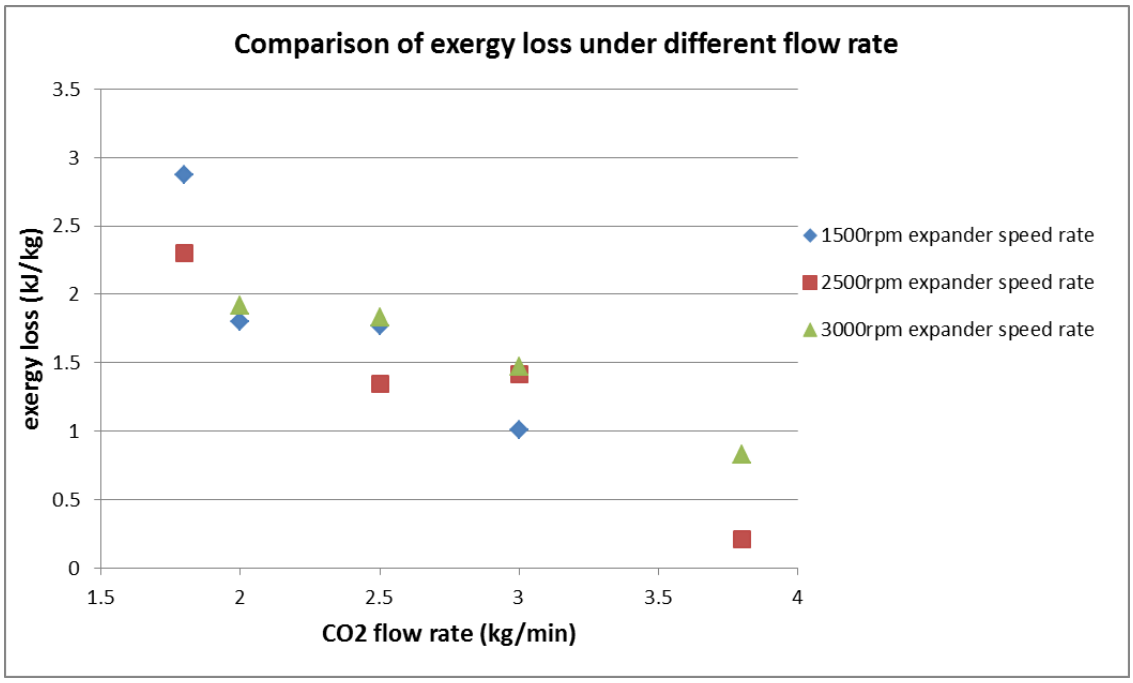

Figure 22 Comparison of total exergy loss under different CO_2 flow rate

From the tables of exergy loss calculation above, it can be concluded that at a fixed expander speed rate, with higher working fluid flow rate comes lower exergy loss. Based on the equation to calculate exergy loss above, in which entropy generation directly determines exergy loss, it is implied that higher entropy generation always leads to higher exergy loss. In principle, for a certain thermal process, the irreversibility of it is measured with either entropy generation or exergy loss. The reasons why higher flow rate can cause lower exergy loss can be inferred that the influence of friction is less contributing to irreversibility, and heat transfer processes in heat exchangers are also more effective under circumstances of high flow rate.

6.2.2 At fixed flow rate

Table 17 Exergy loss (kJ/kg) at 3.5kg/min flow rate of the expander loop

expander speed	HX-2	turbine	HX-3	pump	sum
2900rpm	28.06733	13.69843	-25.6464	-4.19328	11.92608
3500rpm	17.93434	12.04704	-25.8998	-3.50208	0.579456

4200rpm	18.17078	11.87885	-26.4672	-3.50208	0.080352

Table 18 Exergy loss (kJ/kg) at 3.8kg/min flow rate of the expander loop

expander speed	HX-2	turbine	HX-3	pump	sum
2900rpm	22.94352	13.19558	-31.1702	-4.21056	0.758304
3500rpm	18.11059	12.91104	-25.8797	-4.40064	0.741312
4500rpm	16.62826	12.13344	-24.5261	-3.66624	0.569376

Overall, exergy loss of the whole closed expander loop is lower when the expander speed rate increases. This phenomenon has something to do with the expansion process in the turbine with consideration of expander speed rate. However, due to the limits of the expander strength, the expander speed rate cannot go beyond proper working condition that it is designed for. Moreover, resulting from the features of CO_2 as the working fluid in this test rig, the special characteristics of super-critical state CO_2 can bring some influences without a doubt. In the expander of test rig, high-pressured and high-temperature CO_2 reached the super-critical phase, making the heat transfer effects quite different to normal common gases or steams, such as propane or water steam. The unfortunate fact is that no proper expanders that are specially designed for super-critical CO_2 can be found or obtained. Therefore, with a traditional common expander embedded in this test rig, the actual performance of super-critical CO_2 cannot appear to be its best.

6.3 Conclusions from the tests

After operating the test system, especially the expander loop functioning as a Rankine cycle using CO_2 as working fluid, series of data and results were collected through the measurement equipment and analyzed by calculation. From the tests we can draw several conclusions judging from the performance of this system.

Firstly, the feasibility of power generation with Rankine cycle using CO_2 as working

fluid and a heat pump to provide a low temperature input heat source was abundantly testified. It is very clear that during the operation of the system, the system did generate a certain level of power by pushing supercritical phase CO_2 of high temperature and high pressure through the expander. With the analysis above, the amount of power generated was determined by several variables including input heat source temperature, pump efficiency, expander speed rate, etc.

Secondly, the turbine efficiency and overall efficiency were calculated and compared under different working conditions varying from low expander speed rate and low CO_2 mass flow rate to high expander speed rate and high CO_2 mass flow rate. The result of the turbine efficiency was decent, considering the expander we use in the proposed system was not specially manufactured for handling trans-critical phase matter. The overall efficiency of the expander loop was a promising result, with a little neglect of heat loss in the heat transfer process of the input heat exchanger. The overall efficiency was theoretically overrated slightly and optimistically, but it still shows a great potential for further research and study.

6.4 Conclusions from the simulation

With consideration of the limits of the real system, a computational model was established using Dymola platform in Modelica language, in order to simulate the system in modeling process. After the validation of this model, the working condition was extended from 80 ℃ to 150-200 ℃, for the sake of examining the potential of this conceptual system of Rankine cycle using CO_2 as working fluid. The results of the simulation proved to be beneficial for analyzing the virtual power generation after the input heat source temperature was raised to a higher level. This shows a bright path for building a better system which has components capable in strength to handle higher pressure and higher temperature of CO_2 working fluid due to the characteristics of CO_2. Although it is just a computational model and incapable of

revealing further quantified results for research, it can still provide useful proof for the assumptions of creating a bigger scaled and more efficient system with this concept.

Bibliography

[1]Zhang, X. R., et al. "Theoretical analysis of a thermodynamic cycle for power and heat production using supercritical carbon dioxide." *Energy* 32.4 pp. 591-599. 2007

[2]Zhang, Xin-Rong, et al. "A feasibility study of CO_2-based Rankine cycle powered by solar energy." *JSME International Journal Series B* 48.3 pp.540-547 2005

[3]Zhang, X. R., et al. "Study of solar energy powered transcritical cycle using supercritical carbon dioxide." *International journal of energy research* 30.14 pp.1117-1129 2006

[4]Cayer, Emmanuel, et al. "Analysis of a carbon dioxide transcritical power cycle using a low temperature source." *Applied Energy* 86.7 pp.1055-1063. 2009

[5]Lakew, Amlaku Abie, Olav Bolland, and Yves Ladam. "Theoretical thermodynamic analysis of Rankine power cycle with thermal driven pump."*Applied Energy* 88.9 pp.3005-3011 2011

[6]Zhang, Xin-Rong, Hiroshi Yamaguchi, and Daisuke Uneno. "Experimental study on the performance of solar Rankine system using supercritical CO_2." *Renewable Energy* 32.15 pp.2617-2628. 2007

[7]Radermacher, Reinhard. "Thermodynamic and heat transfer implications of working fluid mixtures in Rankine cycles." *International Journal of Heat and Fluid Flow* 10.2 pp.90-102. 1989

[8]Walnum, Harald Taxt, et al. "Off-design operation of ORC and CO_2 power production cycles for low temperature surplus heat recovery." *International Journal of Low-Carbon Technologies* 6.2 pp.134-140. 2011

[9]Kim, Dong-Seon, and CA Infante Ferreira. *Solar absorption cooling*. Vol. 68. No. 04. 2007.

[10]Elliott, Thomas C. "Standard handbook of powerplant engineering." (1989).

[11]Larjola, J. "Electricity from industrial waste heat using high-speed organic Rankine cycle (ORC)." *International journal of production economics* 41.1 (1995): 227-235.

[12]Cengel, Yunus A., and Michael A. Boles. *Thermodynamics: an engineering approach*. Vol. 5. New York: McGraw-Hill, 2011.

[13]Moisseytsev, Anton, and James J. Sienicki. "Investigation of alternative layouts for the supercritical carbon dioxide Brayton cycle for a sodium-cooled fast reactor." *Nuclear Engineering and Design* 239.7 (2009): 1362-1371.

[14]DTU, "CoolPack".

[15]Sergio Girotto, Silvia Minetto, and Petter Neksa. “Commercial refrigeration system using CO_2 as the refrigerant.” *International journal of Refrigeration* 27 (2004): 717-723.

[16]H.M. Getu, P.K. Bansal. “Thermodynamic analysis of an R744-R717 cascade refrigeration system.” *International journal of Refrigeration* 31 (2008): 45-54.

[17]Krzysztof Banasiak, Armin Hafner, Trond Andreson. “Experimental and numerical investigation of the influence of the two-phase ejector geometry on the performance of the R744 heat pump.” *International journal of Refrigeration* 35 (2012): 1617-1625.

[18]Man-Hoe Kim, Jostein Petterson, Clark W. Bullard. “Fundamental process and system design issues in CO_2 vapor compression systems.” *Progress in Energy and*

Combustion Science 30 (2004) 119-174.

[19]Pradeep Bansal. "A review-Status of CO_2 as a low temperature refrigerant: Fundamentals and R&D opportunities." *Applied Thermal Engineering* 41 (2012) 18-29.

[20]Alessandro da Silva, Enio-Pedone Bandarra Filho, Arthur Heleno Pontes Antunes. "Comparison of a R744 cascade refrigeration system with R404A and R22 conventional systems for supermarkets." *Applied Thermal Engineering* 41 (2012) 30-35.

[21]Brian T. Austin, K. Sumathy. "Transcritical carbon dioxide heat pump systems: A review." *Renewable and Sustainable Energy Reviews* 15 (2011) 4013-4029.

[22]Bancha Kongtragool, Somchai Wongwises. "A review of solar-powered Stirling engines and low temperature differential Stirling engines." *Renewable and Sustainable Energy Reviews* 7 (2003) 131-154.

[23]D. Mills. "Advances in solar thermal electricity technology." *Solar Energy* 76 (2004) 19-31.

[24]J. Larjola. "Electricity from industrial waste heat using high-speed organic Rankine cycle (ORC)." *Int. J. Production Economics* 41 (1995) 227-235.

[25]A. Schuster, S. Karellas, E. Kakaras, H. Spliethoff. "Energetic and economic investigation of Organic Rankine Cycle applications." *Applied Thermal Engineering* 29 (2009) 1809-1817.